TECHNICAL REPORT

ISO/TR 1281-2

First edition
2008-12-01

Rolling bearings — Explanatory notes on ISO 281 —

Part 2: **Modified rating life calculation, based on a systems approach to fatigue stresses**

Roulements — Notes explicatives sur l'ISO 281 —

Partie 2: Calcul modifié de la durée nominale de base fondé sur une approche système du travail de fatigue

Reference number
ISO/TR 1281-2:2008(E)

ISO copyright office
Case postale 56 • CH-1211 Geneva 20
Tel. + 41 22 749 01 11
Fax + 41 22 749 09 47
E-mail copyright@iso.org
Web www.iso.org

Published in Switzerland

Contents

Page

Foreword

ISO (the International Organization for Standardization) is a worldwide federation of national standards bodies (ISO member bodies). The work of preparing International Standards is normally carried out through ISO technical committees. Each member body interested in a subject for which a technical committee has been established has the right to be represented on that committee. International organizations, governmental and non-governmental, in liaison with ISO, also take part in the work. ISO collaborates closely with the International Electrotechnical Commission (IEC) on all matters of electrotechnical standardization.

International Standards are drafted in accordance with the rules given in the ISO/IEC Directives, Part 2.

The main task of technical committees is to prepare International Standards. Draft International Standards adopted by the technical committees are circulated to the member bodies for voting. Publication as an International Standard requires approval by at least 75 % of the member bodies casting a vote.

In exceptional circumstances, when a technical committee has collected data of a different kind from that which is normally published as an International Standard ("state of the art", for example), it may decide by a simple majority vote of its participating members to publish a Technical Report. A Technical Report is entirely informative in nature and does not have to be reviewed until the data it provides are considered to be no longer valid or useful.

Attention is drawn to the possibility that some of the elements of this document may be the subject of patent rights. ISO shall not be held responsible for identifying any or all such patent rights.

ISO/TR 1281-2 was prepared by Technical Committee ISO/TC 4, *Rolling bearings*, Subcommittee SC 8, *Load ratings and life*.

This first edition of ISO/TR 1281-2, together with the first edition of ISO/TR 1281-1, cancels and replaces the first edition of ISO/TR 8646:1985, which has been technically revised.

ISO/TR 1281 consists of the following parts, under the general title *Rolling bearings — Explanatory notes on ISO 281*:

— *Part 1: Basic dynamic load rating and basic rating life*

— *Part 2: Modified rating life calculation, based on a systems approach of fatigue stresses*

Introduction

Since the publication of ISO 281:1990 [25], more knowledge has been gained regarding the influence on bearing life of contamination, lubrication, fatigue load limit of the material, internal stresses from mounting, stresses from hardening, etc. It is therefore now possible to take into consideration factors influencing the fatigue load in a more complete way.

Practical implementation of this was first presented in ISO 281:1990/Amd.2:2000, which specified how new additional knowledge could be put into practice in a consistent way in the life equation. The disadvantage was, however, that the influence of contamination and lubrication was presented only in a general fashion. ISO 281:2007 incorporates this amendment, and specifies a practical method of considering the influence on bearing life of lubrication condition, contaminated lubricant and fatigue load of bearing material.

In this part of ISO/TR 1281, background information used in the preparation of ISO 281:2007 is assembled for the information of its users, and to ensure its availability when ISO 281 is revised.

For many years the use of basic rating life, L_{10}, as a criterion of bearing performance has proved satisfactory. This life is associated with 90 % reliability, with commonly used high quality material, good manufacturing quality, and with conventional operating conditions.

However, for many applications, it has become desirable to calculate the life for a different level of reliability and/or for a more accurate life calculation under specified lubrication and contamination conditions. With modern high quality bearing steel, it has been found that, under favourable operating conditions and below a certain Hertzian rolling element contact stress, very long bearing lives, compared with the L_{10} life, can be obtained if the fatigue limit of the bearing steel is not exceeded. On the other hand, bearing lives shorter than the L_{10} life can be obtained under unfavourable operating conditions.

A systems approach to fatigue life calculation has been used in ISO 281:2007. With such a method, the influence on the life of the system due to variation and interaction of interdependent factors is considered by referring all influences to the additional stress they give rise to in the rolling element contacts and under the contact regions.

Rolling bearings — Explanatory notes on ISO 281 —

Part 2: Modified rating life calculation, based on a systems approach to fatigue stresses

1 Scope

ISO 281:2007 introduced a life modification factor, a_{ISO}, based on a systems approach to life calculation, in addition to the life modification factor for reliability, a_1.These factors are applied in the modified rating life equation

$$L_{n\text{m}} = a_1 \, a_{\text{ISO}} \, L_{10} \tag{1}$$

For a range of reliability values, a_1 is given in ISO 281:2007 as well as the method for evaluating the modification factor for systems approach, a_{ISO}. L_{10} is the basic rating life.

This part of ISO/TR 1281 gives supplementary background information regarding the derivation of a_1 and a_{ISO}.

NOTE The derivation of a_{ISO} is primarily based on theory presented in Reference [5], which also deals with the fairly complicated theoretical background of the contamination factor, e_{C}, and other factors considered when calculating a_{ISO} .

2 Normative references

The following referenced documents are indispensable for the application of this document. For dated references, only the edition cited applies. For undated references, the latest edition of the referenced document (including any amendments) applies.

ISO 281:2007, *Rolling bearings — Dynamic load ratings and rating life*

ISO 11171, *Hydraulic fluid power — Calibration of automatic particle counters for liquids*

3 Symbols

Certain other symbols are defined on an *ad hoc* basis in the clause or subclause in which they are used.

A scaling constant in the derivation of the life equation

a_{ISO} life modification factor, based on a systems approach to life calculation

a_{SLF} stress-life factor in Reference [5], based on a systems approach to life calculation (same as the life modification factor a_{ISO} in ISO 281)

a_1 life modification factor for reliability

C basic dynamic load rating, in newtons

C_{u} fatigue load limit, in newtons

C_0 basic static load rating, in newtons

c exponent in the stress-life equation (in Reference [5] and ISO 281, $c = 31/3$ is used)

D_{pw} pitch diameter, in millimetres, of ball or roller set

dV elementary integration volume, in cubic millimetres

e Weibull's exponent (10/9 for ball bearings and 9/8 for roller bearings)

e_C contamination factor

F_r bearing radial load (radial component of actual bearing load), in newtons

L_n life, corresponding to n percent probability of failure, in million revolutions

L_{nm} modified rating life, in million revolutions

L_{we} effective roller length, in millimetres, applicable in the calculation of load ratings

L_{10} basic rating life, in million revolutions

N number of load cycles

n probability of failure, expressed as a percentage

P dynamic equivalent load, in newtons

P_u fatigue load limit, in newtons (same as C_u)

Q_{max} maximum load, in newtons, of a single contact

Q_u fatigue load, in newtons, of a single contact

Q_0 maximum load, in newtons, of a single contact when bearing load is C_0

S reliability (probability of survival), expressed as a percentage

s uncertainty factor

w exponent in the load-stress relationship (1/3 for ball bearings and 1/2,5 for roller bearings)

x contamination particle size, in micrometres, with ISO 11171 calibration

Z number of rolling elements per row

α nominal contact angle, in degrees

β_{cc} lubricant cleanliness degree (in Reference [5] and Clause 5)

$\beta_{x(c)}$ filtration ratio at contamination particle size x (see symbol x above)

NOTE The designation (c) signifies that the particle counters — of particles of size x µm — shall be an APC (automatic optical single-particle counter) calibrated in accordance with ISO 11171.

η_b lubrication factor

η_c contamination factor (same as the contamination factor e_C in ISO 281)

κ viscosity ratio, ν / ν_1

Λ ratio of oil film thickness to composite surface roughness

ν actual kinematic viscosity, in square millimetres per second, at the operating temperature

ν_1 reference kinematic viscosity, in square millimetres per second, required to obtain adequate lubrication

τ_i fatigue stress criterion of an elementary volume, dV, in megapascals

τ_u fatigue stress limit in shear, in megapascals

4 Life modification factor for reliability, a_1

4.1 General

In the context of bearing life for a group of apparently identical rolling bearings, operating under the same conditions, reliability is defined as the percentage of the group that is expected to attain or exceed a specified life.

The reliability of an individual rolling bearing is the probability that the bearing will attain or exceed a specified life. Reliability can thus be expressed as the probability of survival. If this probability is expressed as S %, then the probability of failure is (100 – S) %.

The bearing life can be calculated for different probability of failure levels with the aid of the life modification factor for reliability, a_1.

4.2 Derivation of the life modification factor for reliability

4.2.1 Two parameter Weibull relationship

Endurance tests, which normally involve batches of 10 to 30 bearings with a sufficient number of failed bearings, can be satisfactorily summarized and described using a two parameter Weibull distribution, which can be expressed

$$L_n = \eta \left[\ln \left(\frac{100}{S} \right) \right]^{1/e} \tag{2}$$

$$n = 100 - S \tag{3}$$

where

- S is the probability, expressed as a percentage, of survival;
- n is the probability, expressed as a percentage, of failure;
- e is the Weibull exponent (set at 1,5 when $n < 10$);
- η characteristic life.

With the life L_{10} (corresponding to 10 % probability of failure or 90 % probability of survival) used as the reference, L_n / L_{10} can be written, with the aid of Equation (2), as

$$L_n = L_{10} \left[\frac{\ln(100/S)}{\ln(100/90)} \right]^{1/e} \tag{4}$$

By including the life modification factor for reliability, a_1, Equation (4) can be written

$$L_n = a_1 L_{10} \tag{5}$$

The life modification factor for reliability, a_1, is then given by

$$a_1 = \left[\frac{\ln(100/S)}{\ln(100/90)} \right]^{1/e} \tag{6}$$

4.2.2 Experimental study of the life modification factor for reliability

References [6], [7], and [8] confirm that the two parameter Weibull distribution is valid for reliabilities up to 90 %. However, for reliabilities above 90%, test results indicate that Equation (6) is not accurate enough.

Figures 1 and 2 are reproduced from Reference [8] and illustrate a summary of the test results from References [6] to [8] and others. In Figure 1, the test results, represented by a reliability factor designated a_{1x}, are summarized. The curves are calculated as mean values of the test results. In Figure 2, $a_{1\mathrm{l}x}$ represents the lower value of the ($\pm 3\sigma$) range confidence limits of reliability of the test results, where σ is the standard deviation.

Figure 1 indicates that all mean value curves have a_{1x} values above 0,05, and Figure 2 confirms that the asymptotic value $a_1 = a_{1\mathrm{l}x} = 0{,}05$ for the life modification factor for reliability is on the safe side.

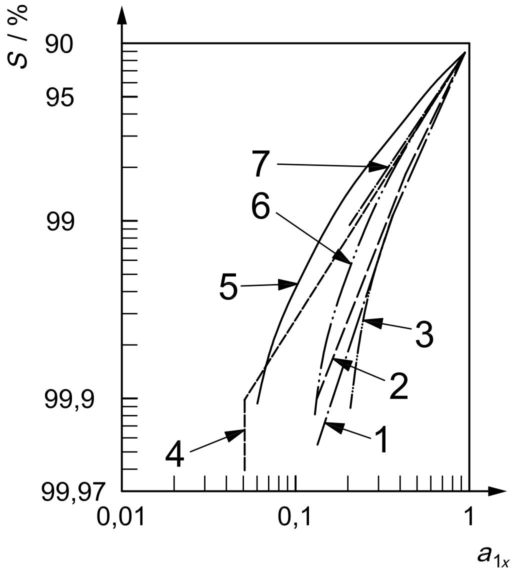

Key

a_{1x} reliability factor
S reliability

1 Reference [8] (total)
2 Reference [8] (ball bearings)
3 Reference [8] (roller bearings)
4 Reference [6]
5 Reference [7]
6 Okamoto et al.
7 ISO 281

Figure 1 — Factor a_{1x}

Reproduced, with permission, from Reference [8]

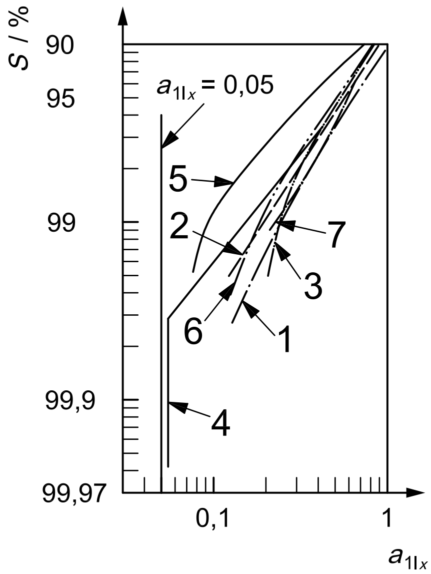

Key

$a_{1\mathrm{l}x}$ lower limit of the $\pm 3\sigma$ confidence range for reliability
S reliability

1 Reference [8] (total)
2 Reference [8] (ball bearings)
3 Reference [8] (roller bearings)
4 Reference [6]
5 Reference [7]
6 Okamoto et al.
7 ISO 281

Figure 2 — Factor $a_{1\mathrm{l}x}$

Reproduced, with permission, from Reference [8]

4.2.3 Three parameter Weibull relationship

The tests (4.2.2) indicate that a three parameter Weibull distribution would better represent the probability of survival for values $>$ 90 %.

The three parameter Weibull relationship is expressed by

$$L_n - \gamma = \eta \left[\ln\left(\frac{100}{S}\right) \right]^{1/e} \tag{7}$$

where γ is the third Weibull parameter.

By introducing a factor C_γ to define γ as a function of L_{10}, γ can be written

$$\gamma = C_\gamma \, L_{10} \tag{8}$$

$$L_n - C_\gamma \, L_{10} = \left(L_{10} - C_\gamma \, L_{10} \right) \left[\frac{\ln(100/S)}{\ln(100/90)} \right]^{1/e} \tag{9}$$

$$L_n = a_1 L_{10} \tag{10}$$

with the new life modification factor for reliability, a_1, defined as

$$a_1 = \left(1 - C_\gamma \right) \left[\frac{\ln(100/S)}{\ln(100/90)} \right]^{1/e} + C_\gamma \tag{11}$$

The factor C_γ represents the asymptotic value of a_1 in Figure 2, i.e. 0,05. This value and a selected Weibull slope, $e = 1{,}5$, give a good representation of the curves in Figure 2. With these values inserted in Equation (11), the equation for the life modification factor for reliability can be written

$$a_1 = 0{,}95 \left[\frac{\ln(100/S)}{\ln(100/90)} \right]^{2/3} + 0{,}05 \tag{12}$$

Table 1 lists reliability factors calculated by Equation (11) for $C_\gamma = 0$ and $e = 1{,}5$, and by Equation (12), along with the life adjustment factor for reliability, a_1, in ISO 281:1990 [25]. The calculations are made for reliabilities, S, from 90 % to 99,95 %.

Values of a_1 calculated by Equation (12) are adopted in ISO 281:2007.

Table 1 — The life modification factor for reliability, a_1, for different Weibull distributions

Reliability S %	**Reliability factor** a_1 ISO 281:1990 [25]	$C_\gamma = 0$ $e = 1,5$	$C_\gamma = 0,05$ $e = 1,5$
90	1	1	1
95	0,62	0,62	0,64
96	0,53	0,53	0,55
97	0,44	0,44	0,47
98	0,33	0,33	0,37
99	0,21	0,21	0,25
99,5	—	0,13	0,17
99,9	—	0,04	0,09
99,95	—	0,03	0,08

Figure 3 shows the probability of failure and the probability of survival as functions of the life modification factor for reliability, a_1, by means of one curve for $C_\gamma = 0$ and $e = 1,5$ and one curve for $C_\gamma = 0,05$ and $e = 1,5$.

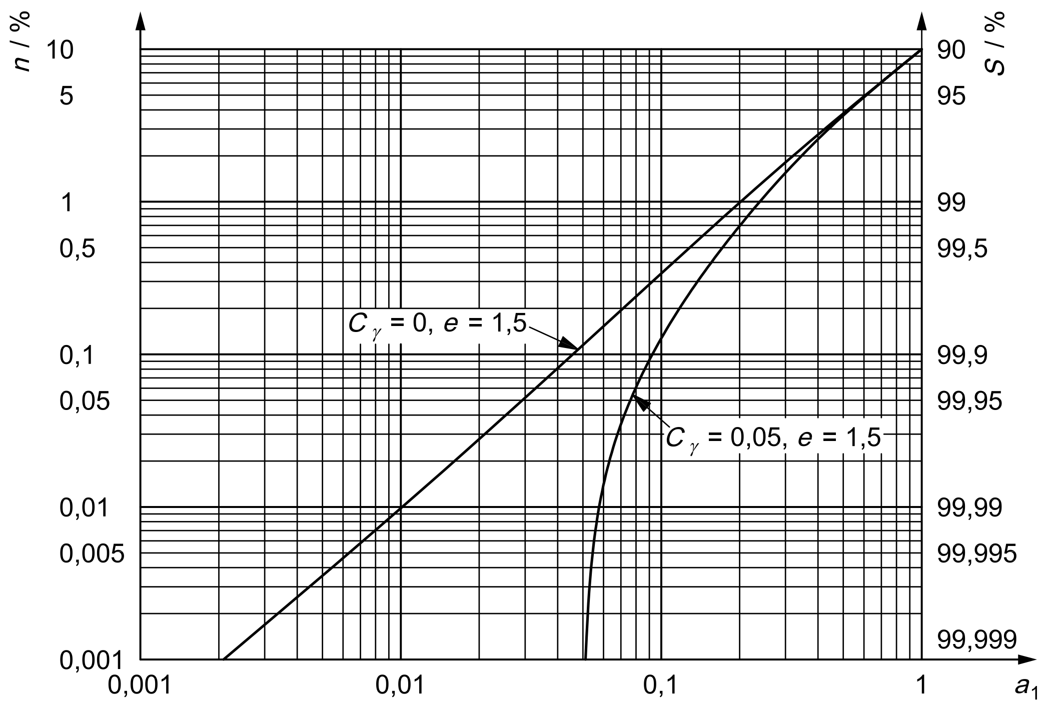

Key

a_1 life modification factor for reliability
C_γ asymptotic value of a_1
e Weibull exponent
n probability of failure
S probability of survival ($S = 100 - n$)

Figure 3 — Weibull distributions with $C_\gamma = 0$ and $C_\gamma = 0,05$

5 Background to the life modification factor, a_{ISO}

5.1 General

The derivation of the life modification factor, a_{ISO}, in ISO 281 is described in Reference [5], where the same factor is called stress-life factor and designated a_{SLF}. In this part of ISO/TR 1281, further information of the derivation of the factor a_{SLF} is given, based on Reference [22].

According to Reference [5], Section 3.2, based on the conditions valid for ISO 281 (i.e. the macro-scale factor $\eta_{\mathrm{a}} = 1$ and $A = 0{,}1$), the equation for a_{SLF} can be written

$$a_{\mathrm{SLF}} = 0{,}1 \left\langle 1 - \left(\eta_{\mathrm{b}} \, \eta_{\mathrm{c}} \frac{P_{\mathrm{u}}}{P} \right)^{w} \right\rangle^{-c/e} \tag{13}$$

The background to the lubrication factor, η_{b}, and the contamination factor, η_{c}, is explained in 5.2 and 5.3 respectively. The contamination factor, η_{c}, corresponds to the factor e_{C} in ISO 281.

5.2 The lubrication factor, η_{b}

This subclause covers the relationship between the lubrication quality, which is characterized by the viscosity ratio, κ, in ISO 281, and its influence on the fatigue stress.

For this purpose, the fatigue life reduction resulting from an actual rolling bearing (with standard raceway surface roughness) compared with one characterized by an ideally smooth contact, as from purely Hertzian, friction-free, stress distribution hypothesis, needs to be quantified.

This can be done by comparing the theoretical fatigue life between a real bearing (with standard raceway surface roughness) and the fatigue life of a hypothetical bearing with ideally smooth and friction-free contacting surfaces. Thus the life ratio of Equation (14) has to be quantified

$$\frac{L_{10,\mathrm{rough}}}{L_{10,\mathrm{smooth}}} = \frac{a_{\mathrm{SLF,rough}}}{a_{\mathrm{SLF,smooth}}} \tag{14}$$

with $(C/P)^p$ constant in the life equation. The ratio in Equation (14) can be evaluated numerically using the Ioannides-Harris fatigue life stress integral of Equation (15) (see Reference [21]):

$$\ln \frac{100}{S} \approx A N^{e} \int_{V_{\mathrm{R}}} \frac{\langle \tau_i - \tau_{\mathrm{u}} \rangle^{c}}{z'^{\,h}} \mathrm{d}V \tag{15}$$

where

h is a depth exponent;

z' is a stress-weighted average depth;

τ represents stress criteria.

In Equation (15), the relevant quantity affecting the life ratio in Equation (14) is the volume-related stress integral I, which can be expressed

$$I = \int_{V_{\mathrm{R}}} \frac{\langle \tau_i - \tau_{\mathrm{u}} \rangle^{c}}{z'^{\,h}} \mathrm{d}V \tag{16}$$

By means of Equations (15) and (16), the life equation can be written

$$L_{10} = 10^{-6} N u^{-1} \approx \left(\frac{\ln(100/90)}{A\, I} \right)^{1/e} u^{-1} \tag{17}$$

The basic rating life in number of revolutions in Equation (17) is expressed as the number of load cycles obtained with 90 % probability, N, divided by the number of over-rolling per revolution, u.

In Equation (17), the stress integral, I, can be computed for both standard roughness and for an ideally smooth contact, and it can be used for estimation of the expected effect of raceway surface roughness on bearing life with the aid of Equations (14) and (17). The following derivation then applies

$$\left(\frac{L_{10,\text{rough}}}{L_{10,\text{smooth}}} \right)_{(m,n)} = \left(\frac{I_{\text{smooth}}}{I_{\text{rough}}} \right)^{1/e}_{(m,n)} = \left(\frac{a_{\text{SLF,rough}}}{a_{\text{SLF,smooth}}} \right)_{(m,n)} \tag{18}$$

In general, this ratio depends on the surface topography (index m) and amount of surface separation or amount of interposed lubricant film (index n).

The lubrication factor can now be directly derived from Equation (18) by introducing the stress-life factor according to Equation (13). For standard-bearing roughness and under the hypothesis of an ideally clean lubricant represented by setting the factor $\eta_{\text{c}} = 1$, the stress-life factor can be written

$$a_{\text{SLF,rough}} = 0{,}1 \left\langle 1 - \left(\eta_{\text{b}} \frac{P_{\text{u}}}{P} \right)^{w} \right\rangle^{-c/e} \tag{19}$$

Similarly, in the case of a well lubricated, hypothetical bearing with ideally smooth surfaces, $\kappa \geqslant 4$, and $\eta_{\text{b}} = 1$ according to the definition of the ranges of η_{b} in Reference [5]. Equation (19) can then be written

$$a_{\text{SLF,smooth}} = 0{,}1 \left\langle 1 - \left(\frac{P_{\text{u}}}{P} \right)^{w} \right\rangle^{-c/e} \tag{20}$$

By inserting Equations (19) and (20) into Equation (18), the following equation is derived

$$\eta_{\text{b}(m,n)} = \frac{P}{P_{\text{u}}} \left\langle 1 - \left\langle 1 - \left(\frac{P_{\text{u}}}{P} \right)^{w} \right\rangle \left(\frac{I_{\text{smooth}}}{I_{\text{rough}}} \right)^{-1/c}_{(m,n)} \right\rangle^{1/w} \tag{21}$$

Equation (21) shows that a ($m \times n$) matrix of numerically derived η_{b} values can be constructed, starting from the calculation of the fatigue life and related stress-volume integral of standard rough bearing raceway surfaces. This calculation has to be extended to include different amounts of surface separation (oil film thickness), from thin films up to full separation in the rolling element/raceway contact.

The following steps were used for the numerical derivation of the $\eta_{\text{b}(m,n)}$, considering actual rolling bearing surfaces.

1) Surface mapping of a variety of rolling bearing surfaces using optical profilometry.

2) Calculation of the operating conditions for the heaviest loaded contact of the bearing.

3) Calculation of the pressure fluctuations resulting from the surface topography, lubrication conditions and resulting elastic deformation by means of the FFT (fast Fourier transform) method.

4) Calculation of the smooth Hertzian stress integral of the contacts using Equation (16).

5) Superimposition of the smooth Hertzian pressure to calculate internal stresses and assessment of the fatigue stress integral of the actual rough contact using Equation (16).

6) Calculation of η_b from Equation (21) in relation to reference operating conditions and resulting viscosity ratio, κ, of the bearing.

Following the methods described above, a set of $\eta_{b(m,\ n)}$ values was constructed. The resulting plots of κ against η_b and interpolation curves are shown in Figure 4. For clarity, only a representative group of standard-bearing raceway surfaces are presented. The generated $\eta_{b(m,\ n)}$ curves show a typical trend with a rapid decline of η_b for a reduction of the nominal lubrication conditions, κ, of the contact.

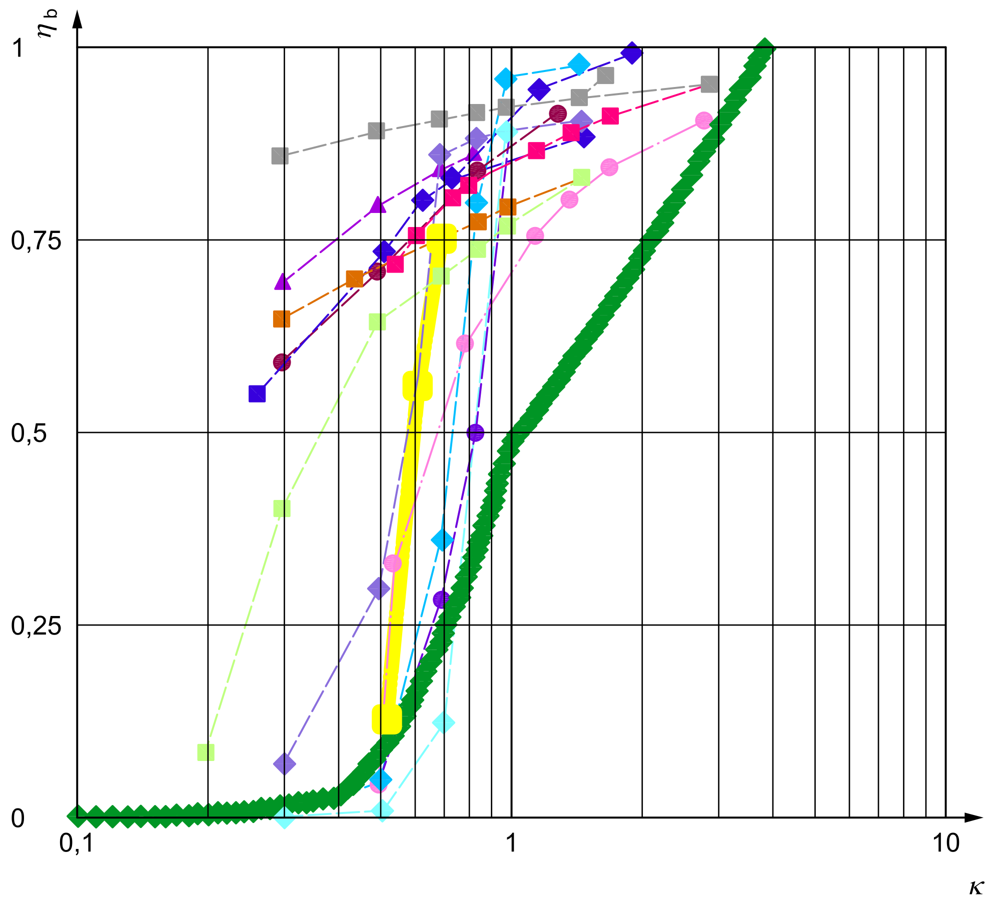

Key

η_b lubrication factor

κ viscosity ratio

Figure 4 — Summary of the numerically calculated lubrication factors for different surface roughness samples compared with the lubrication factor used in ISO 281 (thick line)

In Figure 4, the numerically calculated lubrication factors for different surface roughnesses are indicated and, for comparison, that used in ISO 281, represented by the thick line. The general form of the equation of this thick line is

$$\eta_b(\kappa)_{nom} = \eta_b \frac{(\kappa)_{brg}}{(\psi)_{brg}} = \left(3{,}387 - \frac{b_1(\kappa)}{\kappa^{b_2(\kappa)}}\right)^{5/2} \qquad (22)$$

The factors $b_1(\kappa)$ and $b_2(\kappa)$ are assigned for three intervals of the κ range and ψ_{brg} is a factor characterizing the four main types of bearing geometries (see Reference [5]). Basically, ψ_{brg} accounts for stress concentration, mainly induced by the macro-geometry (such as geometrical precision of the bearing components) and the parasitic effects of the bearing kinematics and resulting dynamics (such as rolling element guidance). Therefore, the determination of the numerical value of ψ_{brg} is essentially experimental. It is based on endurance testing of bearing population samples, similar to the reduction factors λ and ν used when calculating the basic dynamic load ratings of radial and thrust ball and roller bearings (see ISO/TR 1281-1[2]).

When compared with the numerically evaluated η_b curves for different surface roughness samples, the thick line in Figure 4 indicates a good safety margin and Equation (22) is a reasonably safe choice for the rating of the lubrication factors that are used in ISO 281.

Equation (22) is described in Reference [5] and resembles closely the basis of the experimentally derived $a_{23}(\kappa)$ graphs used in bearing manufacturers' catalogues for several years.

5.3 The contamination factor, η_c

The contamination factor designated e_C in ISO 281 is the same as the contamination factor η_c.

The same basic methodology used in the assessment of the lubrication factor can also be applied when assessing the contamination factor. As with the lubrication factor, quantification of the fatigue life resulting from a rolling bearing with dented raceways is required. This fatigue life has to be compared with the life of a bearing characterized by ideally smooth rolling contacts (smooth life integral).

Thus, the following life ratio has to be quantified:

$$\left(\frac{L_{10,\text{dented}}}{L_{10,\text{smooth}}}\right)_{(m,n,i)} = \left(\frac{I_{\text{smooth}}}{I_{\text{dented}}}\right)^{1/e}_{(m,n,i)} = \left(\frac{a_{\text{SLF,dented}}}{a_{\text{SLF,smooth}}}\right)_{(m,n,i)} \tag{23}$$

As from the earlier analyses, the above ratio can be evaluated numerically using the Ioannides-Harris fatigue integral. This ratio is assumed to be dependent of the amount of surface denting (indicated by the index m), the size of the Hertzian contact (indicated by the index n) and amount of oil interposed in the rolling element/raceway contact (indicated by the index i).

In order to limit the complexity of the analysis, the effect of localized stress intensification is decoupled from dents (assumed to be the dominating effect) and the overall roughness-induced stress — thus $\eta_b = 1$.

The stress-life factor according to Equation (13) for a standard bearing under the hypothesis that contamination particle-induced denting is the predominant effect can be written as

$$a_{\text{SLF,dented}} = 0{,}1\left\langle 1-\left(\eta_c \frac{P_u}{P}\right)^{w}\right\rangle^{-c/e} \tag{24}$$

Similarly, for a bearing without surface denting, the contamination factor can be set to $\eta_c = 1$ and the stress-life factor be written

$$a_{\text{SLF,smooth}} = 0{,}1\left\langle 1-\left(\frac{P_u}{P}\right)^{w}\right\rangle^{-c/e} \tag{25}$$

Inserting Equations (24) and (25) into Equation (23) yields:

$$\eta_{\text{c}(m,n,i)} = \frac{P}{P_\text{u}} \left\langle 1 - \left\langle 1 - \left(\frac{P_\text{u}}{P} \right)^w \right\rangle \times \left(\frac{I_\text{smooth}}{I_\text{dented}} \right)_{(m,n,i)}^{-1/c} \right\rangle^{1/w} \tag{26}$$

Equation (26) shows that a matrix (m, n, i) of numerically derived values of η_c can be constructed starting from the numerical calculation of the volume-related fatigue-stress integral, computed considering different amounts of contamination denting on a number of different bearing raceways.

Also, in this case, matrix construction can be accomplished by using the Ioannides-Harris rolling contact fatigue life Equation (15) for the calculation of the volume-related stress integral, Equation (16), for different rolling element/raceway contacts. Basically, the life ratio of Equation (23) has to be evaluated to represent bearings exposed to lubricants with different amounts of contamination particles.

In order to carry out this calculation, it is required to have a measure of the population of dents that are found on typical raceways of bearings exposed to lubricant with various degrees of particle contamination. Statistical measurement of the dent population found on the bearing raceways can provide a direct representation of the effect of a given oil cleanliness and related operating conditions.

The numerically calculated stress integral of the dented region is the parameter that characterizes the contamination factor of Equation (26). As illustrated in Figure 5, the magnitude and distribution of the stress rise at the dent from a given dent geometry is strongly affected by the lubricant film present at the dent. Thicker lubricant films will result in a reduction (damping) and redistribution of contact stress developed at the dent, while a negligible film thickness will sharpen the stress concentration and raise the stress to its maximum.

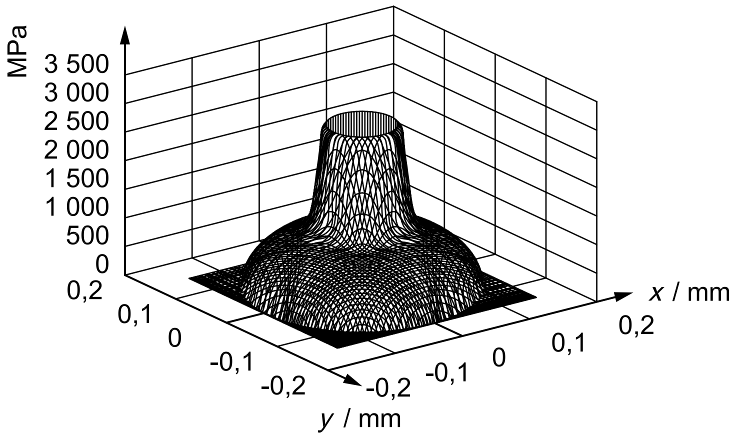

a)

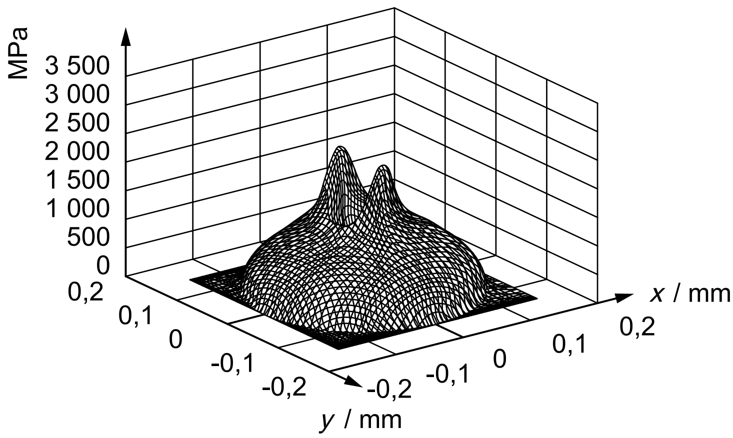

b)

Key

y direction

x direction

Figure 5 — Example of over-rolling contact pressure calculations of simplified dent geometry (150 µm diameter and 5 µm depth) under dry and lubricated conditions: a) contact stress under dry condition (no lubricant film); b) same dent showing the contact stress attenuation induced by a 0,55 µm oil film present in the rolling contact

The size of the bearing has an effect on the life ratio in Equation (23). Large bearings will have a large smooth stress integral, which will have a dominant effect over the dent stress integral. Large diameter bearings therefore have an advantage in terms of the life modification factor.

By solving Equation (26) for a number of different dent topographies found on bearing raceways, a tool for the theoretical evaluation of the η_c factor is made available.

Results of this analysis can be compared to using simplified standard plots for calculation of the contamination factor, η_c, based on the Equations (27) and (28). These equations are used for calculation of the contamination factor, e_C, in ISO 281, which is the same as the η_c factor.

$$\eta_c\left(\kappa, D_{pw}\right)_{\beta_{cc}} = K \qquad (27)$$

$$K = \min\left[C_1\left(\beta_{cc}\right)\kappa^{0,68} D_{pw}{}^{0,55}, 1\right]\left\{1 - \left[C_2\left(\beta_{cc}\right) D_{pw}{}^{-1/3}\right]\right\} \tag{28}$$

where the factors C_1 and C_2 have constant values determined by the oil cleanliness classification, β_{cc}, based on ISO 4406 [3] cleanliness codes or, alternatively, an equivalent filtration ratio $\beta_{x(c)}$ for on-line filtered circulating oil. For grease lubrication, β_{cc} is based on an estimated level of contamination.

As distinguished from the η_b model, the η_c model depends on three variables and therefore a comparison of the theoretical model of η_c, based on Equation (26), while the ISO 281 model, based on Equations (27) and (28), is more complicated.

Two cases calculated with the same extremes of cleanliness and size are compared in Figures 6 and 7.

In Figure 6, the calculation has been made under an on-line filtration condition for bearings of the same size, $D_{pw} = 50$ mm, but under two extreme cleanliness conditions. The cleanliness level used in the numerical calculation with Equation (26) and by use of the e_C graphs in ISO 281 corresponds to the ISO 4406:1999[3] codes —/13/10 and —/19/16.

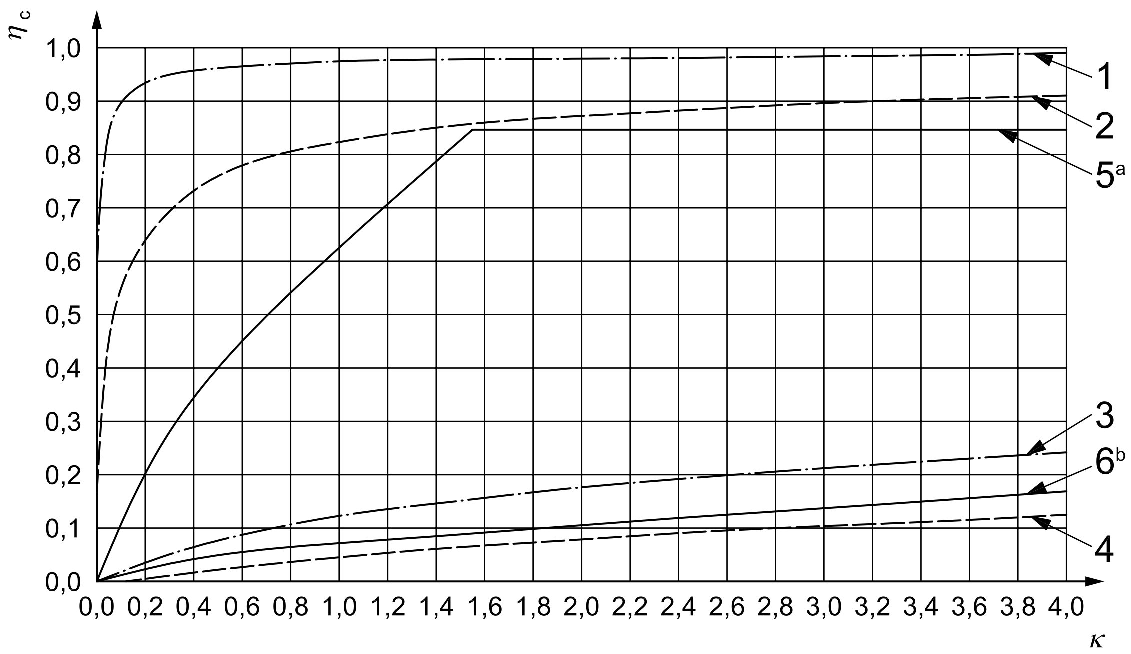

Key

η_c contamination factor 1 and 2, 3 and 4 result ranges for numerically derived contamination factor

κ viscosity ratio 5, 6 contamination factor equivalent to the e_C curve in ISO 281

NOTE Pitch diameter of the bearing is 50 mm.

a High cleanliness (ISO 4406:1999[3] —/13/10).

b Severe contamination (ISO 4406:1999[3] —/19/16).

Figure 6 — Comparison of the numerically derived contamination factor (discontinuous lines) **and the contamination factor equivalent to the e_C graph in ISO 281** (solid lines) **for on-line filtration with the bearing operating under high cleanliness and severe contamination**

In Figure 7 the calculation has been made under an oil bath condition for two different extreme bearing sizes, $D_{pw} = 2\,000$ mm and $D_{pw} = 25$ mm. The oil cleanliness level used in the numerical calculations with Equation (26) and by use of the e_C graphs in ISO 281 corresponds to the mean value of the range between ISO 4406:1999[3] —/15/12 and —/17/14.

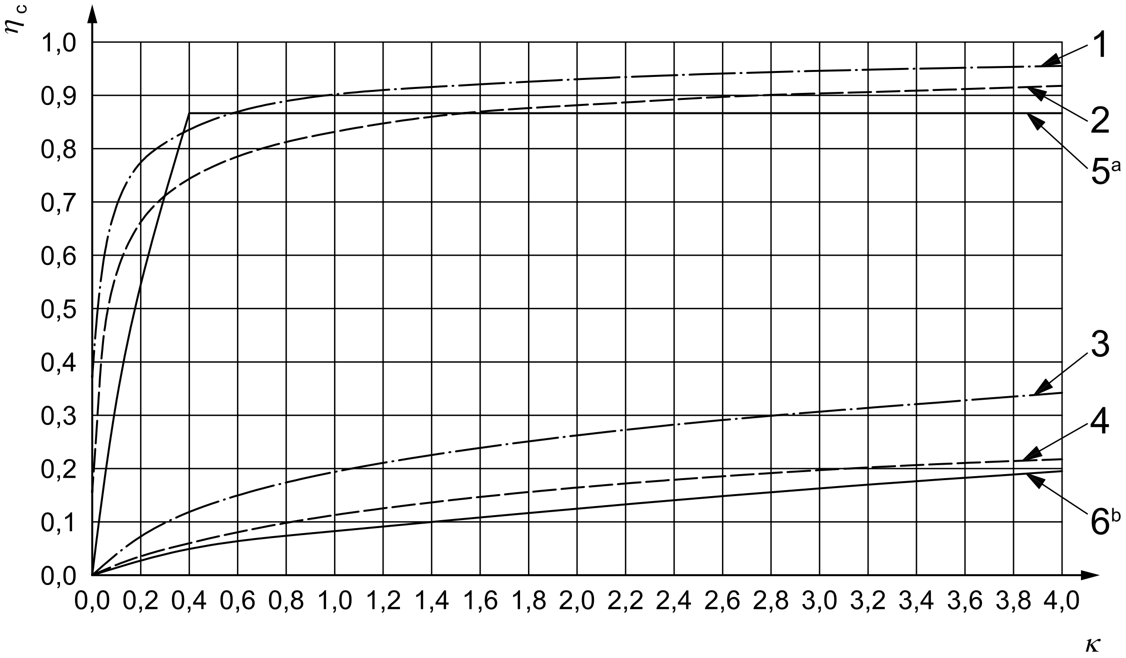

Key

η_c contamination factor 1 and 2, 3 and 4 result ranges for numerically derived contamination factor

κ viscosity ratio 5, 6 contamination factor equivalent to the e_C curves in ISO 281

a $D_{pw} = 2\ 000$ mm.

b $D_{pw} = 25$ mm.

Figure 7 — Comparison of the numerically derived contamination factor (discontinuous lines) **and the contamination factor equivalent to the e_C graphs in ISO 281** (solid lines) **for oil bath lubrication with the bearing operating under a cleanliness level corresponding to the mean value of the range between ISO 4406:1999[3] —/15/12 and —/17/14**

The numerically calculated $\eta_{C(m,n,i)}$ results and the η_C values based on the ISO 281 graphs indicate good correlation in the Figures 6 and 7 with the values from the ISO 281 graphs slightly on the safe side. These graphs show good ability to reproduce the response of the theoretical model, Equation (26), with regard to cleanliness ratings of the lubricant, Figure 6, and the diameter variation, Figure 7.

Regarding the functional dependency of the e_C values from ISO 281, the following can be observed:

a) for high κ values, the ISO 281 model displays a good correlation with the theory;

b) for the low κ range, the ISO 281 model response applies, and in some cases results in a more conservative estimation of the contamination factor.

However, it can be observed that it is indeed in the low κ range that the theoretical model has greater uncertainty, as it is based on a simple nominal lubricant film thickness, while the failure mechanism is mainly a local event. Thus, the conservative approach adopted by ISO 281 seems justified.

5.4 Experimental results

5.4.1 General

Endurance testing of bearings subjected to predefined contamination conditions is not a simple undertaking. There are many difficulties in simulating in a test environment the type of over-rolling dent patterns and dent damage that is expected in a standard industrial application, e.g. a gearbox, characterized by a given ISO 4406[3] oil cleanliness code.

For instance, in a test environment, the lubricant reservoir can be much larger than in a normal bearing application. Moreover, the way the oil is flushed through the bearing may significantly differ from what generally occurs in an actual bearing application.

Thus, in setting up the test conditions, the actual total number of particles that reach the test bearing and that are over-rolled has to be considered as a contamination reference. This is done to avoid excessive dent damage that would misrepresent the typical or conventional use of rolling bearings. Furthermore, the contamination level is the result of the balance between any contaminant originally present in the system and the particles that are generated in and removed from the circulating oil.

These difficulties, among others, have hindered previous attempts to use purely experimental methods in the development of a contamination factor for bearing life ratings. Nevertheless, endurance testing under different oil contamination conditions has been performed in the past, and a significant number of test results have become available. It is therefore possible to compare the response of the ISO 281 contamination factor with these life tests.

Basically, the cleanliness conditions used in bearing life testing can be categorized in three classes (5.4.2 to 5.4.4).

5.4.2 Standard-bearing life tests

The primary purpose is to test bearing life; testing is performed with good oil filtration provided by means of a multi-pass high efficiency system with $\beta_{x(\mathrm{c})} = 3$ (or better). With this filtration, cleanliness codes ISO 4406:1999[3] —/13/10 to —/14/11 can be expected. Considering the mean diameter range of the bearings tested, the expected e_C factor, resulting from this type of testing with full film lubrication, is 0,8 to 1.

5.4.3 Tests with sealed bearings

In this bearing life test, contaminated oil flows around a sealed bearing. The oil is pre-contaminated with a fixed quantity of hard (~750 HV) metallic particles. Contamination particles normally have a size distribution of 25 µm to 50 µm.

The bearing seals provide a filtering action through which only a limited quantity of small sized particles are able to penetrate and hence contaminate the bearing. This type of test can be rated as slight contamination (oil bath ISO 4406:1999[3] codes —/15/12 to —/16/13). Under the given test conditions, the expected e_C factor for this type of testing is 0,3 to 0,5.

5.4.4 Pre-contaminated tests

The test starts with a 30 min run-in with an oil circulation system, which is contaminated with a fixed quantity of hard (~750 HV) metallic particles (size range 25 µm to 50 µm). After this run-in time under contamination conditions, the bearing is tested under standard clean conditions.

This procedure has been shown to be very effective in producing a repeatable dent pattern, i.e. predefined denting on the bearing raceways. Under the given test conditions, this type of test is rated as typical to severe contamination (oil bath ISO 4406:1999[3] codes —/17/14 to —/19/15). The expected e_C factor for this type of endurance test is 0,01 to 0,3.

5.4.5 Evaluation of test results

The contamination factor is obtained from the experimentally derived L_{10} value so as to get the best possible representation of the limited number of test data. The experimentally derived contamination factors are then compared with the ISO 281 e_C curves.

This comparison is shown in Figures 8 to 10. The figures indicate that the experimental data points (given the nature of endurance test data that was available) are limited in number and thus unable to show a clear trend line when compared with the e_C curves. Nevertheless, a good match can be discerned between the average values of the points related to the three different cleanliness classifications and the related e_C curves from ISO 281. Indeed, the trend lines fitted from the experimental data points are well in line with the corresponding e_C curves for all cases that were examined.

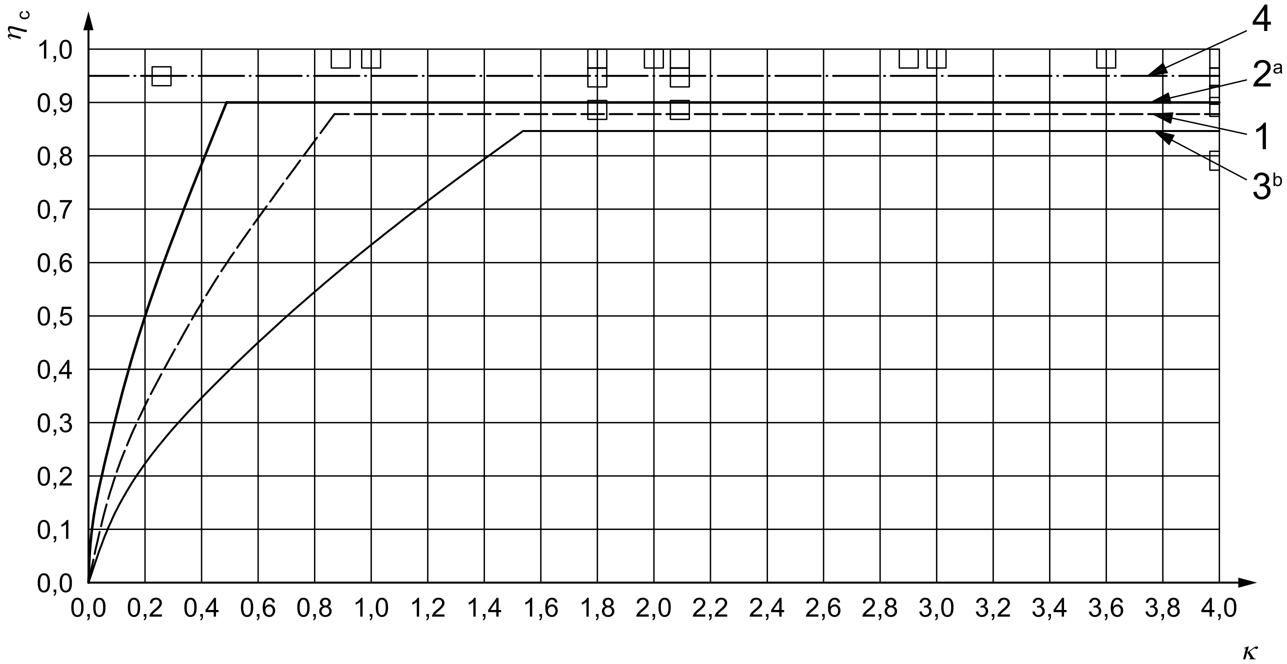

Key

η_c contamination factor

κ viscosity ratio

□ bearing life test data points

1 trend curve for lines 2 and 3

2, 3 border lines of the range, equivalent to those of ISO 281, based on on-line filtration with cleanliness ranges ISO 4406:1999[3] —/13/10 to —/14/11

4 trend line for the bearings tested (curve fit of the experimental data points)

a D_{pw} = 200 mm.

b D_{pw} = 50 mm.

Figure 8 — Comparison of contamination factors obtained from bearing life testing with an η_c (e_C) curve range from ISO 281

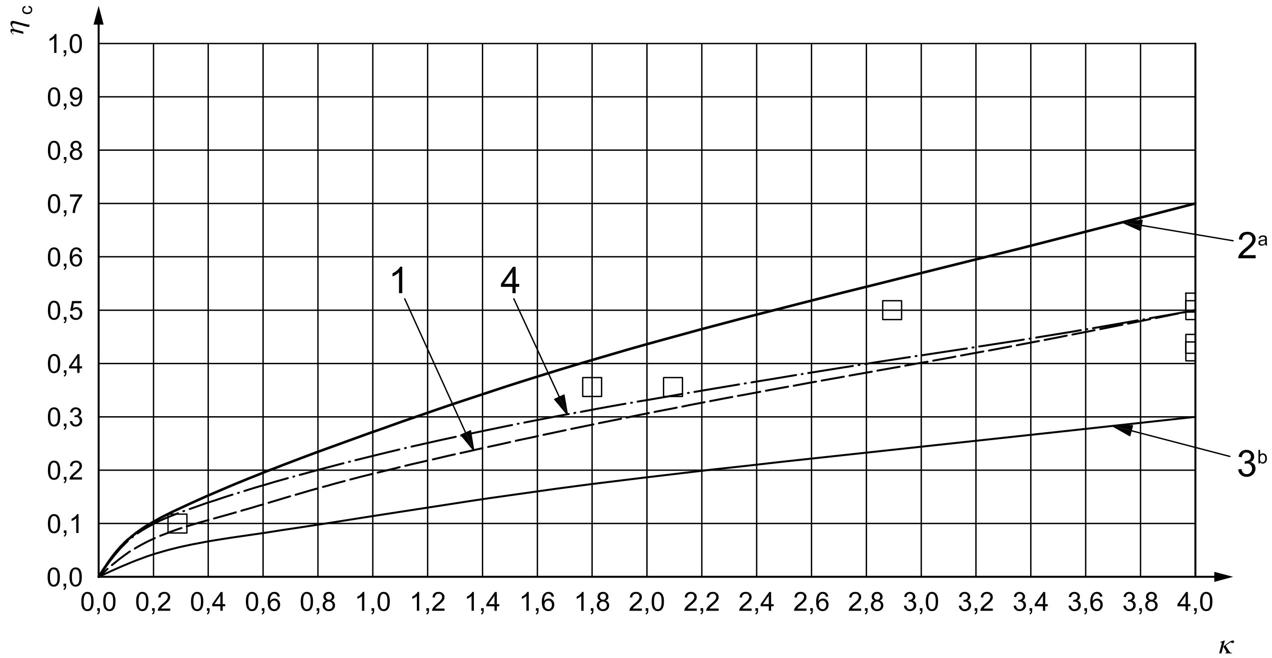

Key

η_c contamination factor

κ viscosity ratio

□ sealed bearing test data points

1 trend curve for lines 2 and 3

2, 3 border lines of the range, equivalent to those of ISO 281, based on oil bath lubrication with cleanliness ranges ISO 4406:1999[3] —/15/12 to —/16/13

4 trend line for the bearings tested (curve fit of the experimental data points, imposing the origin)

a $D_{pw} = 100$ mm.

b $D_{pw} = 30$ mm.

Figure 9 — Comparison of contamination factors obtained from sealed bearing testing with an η_c (e_C) curve range from ISO 281

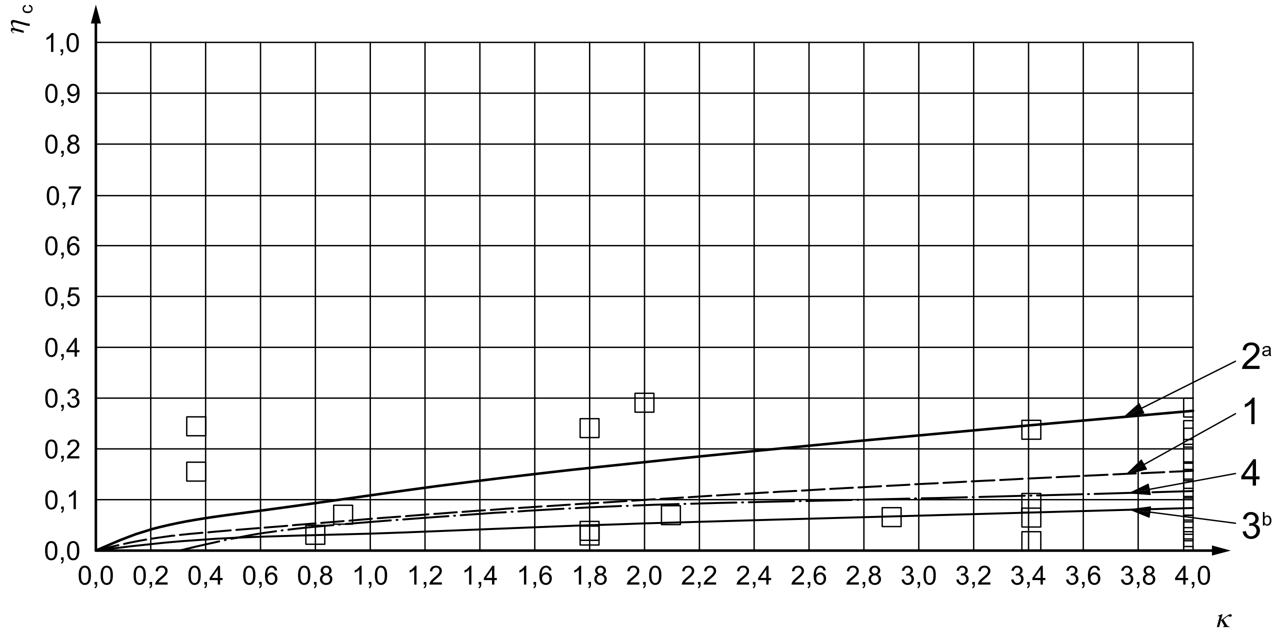

Key

η_c contamination factor

κ viscosity ratio

□ pre-contaminated run-in bearing test data points

1 trend curve for lines 2 and 3

2, 3 border lines of the range, equivalent to those of ISO 281, based on pre-contaminated run-in bearings, comparable to cleanliness ranges ISO 4406:1999[3] —/17/14 to —/19/15

4 trend line for the bearings tested (curve fit of the experimental data points, imposing the origin)

[a] $D_{pw} = 100$ mm.

[b] $D_{pw} = 25$ mm.

Figure 10 — Comparison of contamination factors obtained from pre-contaminated run-in bearing testing with an η_c (e_C) curve range from ISO 281

It is also clear that a detailed evaluation of the model response based only on experimental data is not possible. A principal difficulty is the limited range of the bearing pitch diameter that is used in bearing life testing. The pitch diameter of life-tested bearings is usually between 50 mm and 140 mm, thus limiting the range for the comparison with the e_C graphs in ISO 281.

Furthermore, all test results here are related to bearings tested at relatively heavy loads $P/C \geqslant 0{,}4$. However, it is known that testing at lower loads (for instance $P/C \ll 0{,}3$) and with a significant amount of high hardness (tough minerals) solid particles can lead to an early development of wear and a significant reduction of the life expectancy. However, this area is not covered as it is considered outside or bordering on the conventional working conditions normally considered within the scope of ISO 281.

5.5 Conclusions

Clause 5 demonstrates that, by combining:

a) advanced calculation tools for the accurate prediction of the stress causing fatigue, i.e. Ioannides-Harris volume-related fatigue integral; and

b) the well-established stress-life factor basic methodology;

a simple theoretical framework can be constructed to guide the evaluation of the lubrication and contamination factors used by ISO 281.

Comparison with experimental results shows that this approach leads to results that are consistent with the observations of upper, lower and intermediate levels of contamination and lubrication conditions.

Moreover, large bearing sizes, which are difficult to test by experiment, can be approached by theoretical numerical calculation. The numerically calculated $\eta_{\mathrm{c}(m,n,i)}$ results and the η_c values based on ISO 281 also indicate good matching for large 2 000 mm bearings in Figure 7.

The theoretical and experimental approach described confirms that a combination of experimental tests and theoretical evaluations has provided a good background for the establishment of the e_C graphs in ISO 281.

5.6 Practical application of the contamination factor according to Reference [5], Equation (19.a)

5.6.1 General

The theoretical and experimental background for establishing the η_c graphs and equations in ISO 281 has been explained in 5.5. The connexion between the complicated final contamination factor in Reference [5], Equation (19.a), and application in ISO 281 is now explained practically.

5.6.2 Reference [5], Equation (19.a)

Reference [5], Equation (19.a), is illustrated in Figure 11. The sketches show from left to right that the contamination factor η_c (which corresponds to the contamination factor e_C in ISO 281), is based on the scaled Hertzian macro-contact area, $\tilde{A}_0$, the scaled micro-contact area, $\tilde{A}_\mathrm{m}(\kappa)$, from surface irregularities, $\Omega_\mathrm{rgh}(\kappa)$, and the indentations from contamination particles, $\Omega_\mathrm{dnt}(D_\mathrm{pw}, \beta_\mathrm{cc})$. D_pw is the bearing pitch diameter of rolling elements and β_cc expresses the degree of cleanliness of the lubricant.

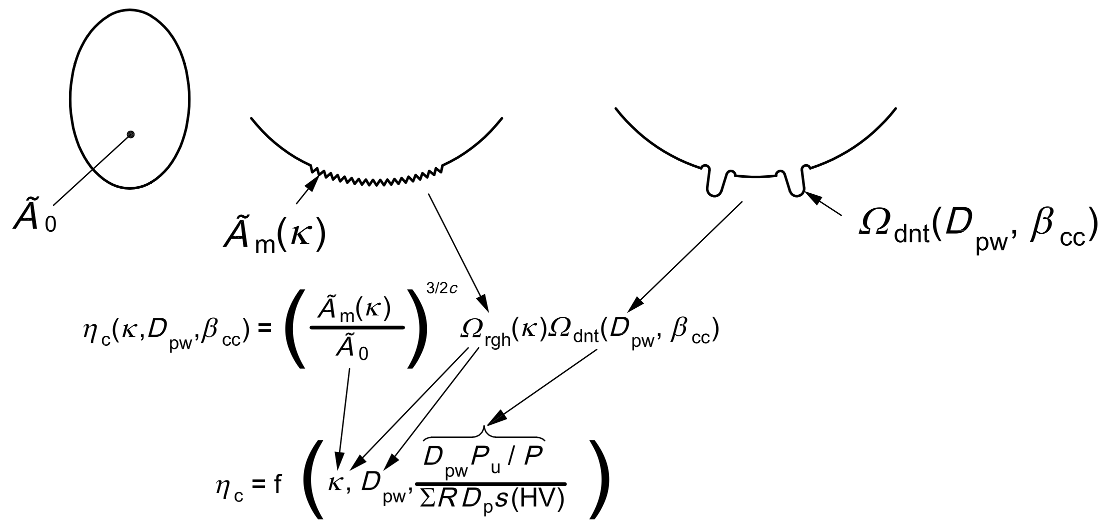

Key

$\tilde{A}_0$	scaled Hertzian macro-contact area
$\tilde{A}_m(\kappa)$	scaled micro-contact area
D_{pw}	bearing pitch diameter
(HV)	contamination particle hardness factor
P	dynamic equivalent load
P_u	fatigue load limit
s	uncertainty factor
β_{cc}	degree of cleanliness of the lubricant
η_c	contamination factor (corresponds to e_c in ISO 281)
κ	viscosity ratio
ΣR	contamination balance factor
$\Omega_{dnt}(D_{pw}, \beta_{cc})$	dent damage expectancy function (indentations from contamination particles)
$\Omega_{rgh}(\kappa)$	bearing asperity micro-stress expectancy function (surface irregularities)

Figure 11 — Reference [5], Equation (19.a)

5.6.3 Scaled micro-contact area divided by scaled macro-contact area

In $[\tilde{A}_m(\kappa)/\tilde{A}_0]^{3/2c}$, the symbols $\tilde{A}_m/\tilde{A}_0$ express the ratio between the micro-contact area and the Hertzian macro-contact area.

In $[\tilde{A}_m(\kappa)/\tilde{A}_0]^{3/2c}$, the ratio $\tilde{A}_m/\tilde{A}_0$ is scaled to fulfil the conditions in Reference [5], Appendix A.6, for the lubrication factor η_b, that is $\eta_b = 1$ for $\kappa = 4$ and $\eta_b = 0$ for $\kappa = 0{,}1$.

The ratio of the scaled contact areas $[\tilde{A}_m(\kappa)/\tilde{A}_0]^{3/2c}$ is evaluated from ordinary asperity contact calculations considering standard rolling bearing roughness and is dependent on the degree of lubrication separation of the surfaces; it is thus related to the viscosity ratio, κ.

The evaluation follows the asperity stress analysis in rolling bearing contacts that can be found in Reference [9]. For the asperity contact calculation, the values for the area reported in Reference [9], surface 2, can be used.

5.6.4 Micro-stress asperity expectancy function

The bearing asperity micro-stress expectancy function related to micro-contact area, $\Omega_{rgh}(\kappa)$, depends on the degree of separation of the contacting surfaces, expressed by κ. The size of the original surface roughness is related to the pitch diameter, D_{pw}, which also has an influence on $\Omega_{rgh}(\kappa)$.

5.6.5 Dent damage expectancy function

5.6.5.1 Derivation

The dent damage expectancy function $\Omega_{\text{dnt}}(D_{\text{pw}}, \beta_{\text{cc}})$ can, in the first instance, be constructed as a simple exponential relationship between the bearing pitch diameter, D_{pw}, the quantity, ΣR, and the size, D_{p}, of the contamination particles entering the bearing.

A contamination balance factor, ΣR, takes into account contamination after mounting, ingress of contamination during operation, contamination produced in the system, and contamination removed from the system.

For an oil bath, the lubrication cleanliness may be given in terms of the cleanliness class according to ISO 4406[3]. In case of oil circulation, the filtering efficiency of the system is also used. This is defined by the filtration ratio $\beta_{x(\text{c})}$.

In the expression for $\Omega_{\text{dnt}}(D_{\text{pw}}, \beta_{\text{cc}})$ in Figure 11, the influence of the uncertainty factor, s, and the contamination particle hardness factor, expressed as (HV), are explained in 5.6.5.2 to 5.6.5.4.

5.6.5.2 Uncertainty factor

For on-line filtered oil lubrication and oil bath lubrication, the selection of e_{C} graphs is made by means of the ISO 4406[3] cleanliness codes.

The disadvantage of these codes is that the maximum particle size recorded is only 15 µm, but most dangerous from a fatigue point of view are the larger particles in the lubricant.

With on-line filters, the filtration ratio, $\beta_{x(\text{c})}$, gives an indication of the expected maximum particle size fairly well. For an oil bath, the measured the ISO 4406[3] code, however, does not provide an indication of the maximum particle size.

It has been found that the maximum particle size is very different for on-line filtered oil and oil bath samples when both have the same ISO 4406[3] code value.

One example is shown in Figure 12, where it can be found that, with on-line filters, the maximum particle size is around 30 µm.

For oil bath lubrication some larger particles were also found.

Tests have been carried out with oils from different bearing applications with different lubrication methods, and the results evaluated. It is, however, important to realize that filtering and particle counting are not accurate science, as is also stated in ISO 281.

A great number of tests were carried out and evaluated, and similar behaviour to that shown in Figure 12 was obtained. This made it possible to apply the same straight lines for oil bath and on-line filtered oils, within the range of the maximum particle size for on-line filtration, when both methods have the same ISO 4406[3] code. The fact that with an oil bath some particles larger than particles obtained with on-line filtration can be expected has, however, also to be considered.

The maximum particle size for oil bath lubrication that can be expected for different ISO 4406[3] codes has been estimated from different test results and considered by means of the uncertainty factor, s, in Figure 11. The influence of the expected larger particles for oil bath lubrication is considered in the e_{C} graphs and equations.

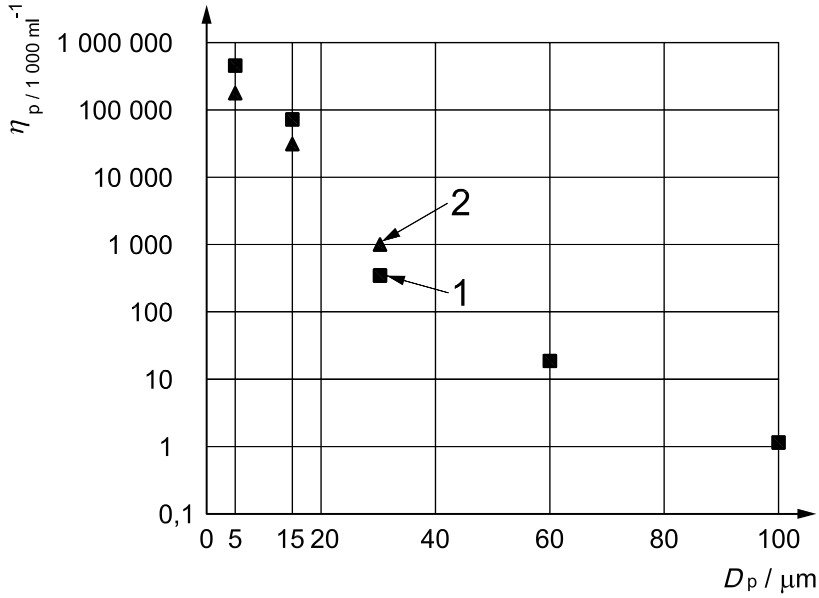

Key

D_p particle size

n_p particle density

1 oil bath

2 on-line filter

Figure 12 — Plot showing measured particle counts, for oil bath and on-line filter lubrication systems

5.6.5.3 Uncertainty factors for heavily contaminated oils by large hard debris particles

Reference [10] lists three parts of a paper in which the influence on bearing life of oil film thickness in the ball/raceway contact of heavily contaminated oils has been studied. To a clean oil bath, a certain quantity of hard 100 µm to 150 µm particles were provided. Particle hardness was 800 HV. During rotation at 2 500 r/min of small deep groove ball bearings, 6206, the oil bath was stirred by compressed air to prevent the particles sinking to the bottom.

The conditions were thus very different from normal conditions in order to make the particle effect clear. In ISO 281, it is assumed that the contamination always consists of a mixture of particles of different size and hardness, where the quantity of small particles dominates. With on-line filtered lubricants, the filter removes the largest particles and only a few particles, slightly larger than the particle size determined by the filtration ratio, pass the filter (see 5.6.5.2).

With oil bath lubrication, the largest particles can also enter the rolling element/raceway contact, even if many large particles sink to the bottom of the oil bath.

The result of Reference [10] indicates that, under test conditions, a thick oil film has a more negative influence on bearing life than a thin oil film, which is contrary to common expectations.

In the new life theory in ISO 281, the bearing life is determined, according to Reference [5], by the Hertzian macro-contact, $[\tilde{A}_m(\kappa)/\tilde{A}_0]^{3/2c}$, the micro-contact, $\Omega_{rgh}(\kappa)$, and the dent damage expectancy function $\Omega_{dnt}(D_{pw}, \beta_{cc})$.

With oil bath lubrication and thin oil film thickness, the influence of the macro-contact, $[\tilde{A}_m(\kappa)/\tilde{A}_0]^{3/2c}$, and the micro-contact, $\Omega_{rgh}(\kappa)$, have large influences on bearing life. With a thick oil film this influence is smaller, but on the other hand the dent damage expectancy function, $\Omega_{dnt}(D_{pw}, \beta_{cc})$, may have a greater influence on thick oil films because of more, and possibly also larger, particles entering the rolling element/raceway contact. For normal dirt conditions in bearing applications, the influence of debris for different oil film thicknesses is balanced as described above in life calculations.

NOTE However, in the test with only a fairly large quantity of large particles, stirred to facilitate constant dirt condition, a thick oil film evidently facilitated the entrance of the large particles. This resulted in more indentations and consequent shorter bearing lives compared with the lives of the thin oil film tests.

For all tests, the bearing lives were much shorter than can be expected with the ISO 281 method (where it is assumed common particle distributions have a maximum size of 150 µm) because of a much larger quantity of large particles entering the ball/raceway contact. The uncertainty factor is thus much larger under the test conditions used.

The test also confirms that the combination oil film thickness, particle size and quantity of particles has a very large influence on bearing life. Different kinds of similar influences can only be dealt with by a systems approach as used in ISO 281. Multiplication factors cannot account for the interrelationship of factors having an influence on bearing fatigue life.

5.6.5.4 Influence on contamination of particle hardness

The e_C graphs in ISO 281 are primarily based on common contamination in bearing applications, that is a mixture of hardened steel particles (700 HV) and softer particles, e.g. from the cage, from the mounting, and from the environment. From the environment, very hard brittle particles (above 700 HV) such as sand can also contaminate the lubricant. These particles are, however, crushed to small particles in the rolling element contacts, and therefore not dangerous from a fatigue point of view.

In a workshop, the environment may contain very hard particles, e.g. carborundum from grinding wheels, which can penetrate the seals and be part of the contamination in the lubricant.

An indication of how dangerous this contamination is when compared with hardened steel contamination can be obtained from the results of theoretical and practical analyses depicted in Figures 13 and 14.

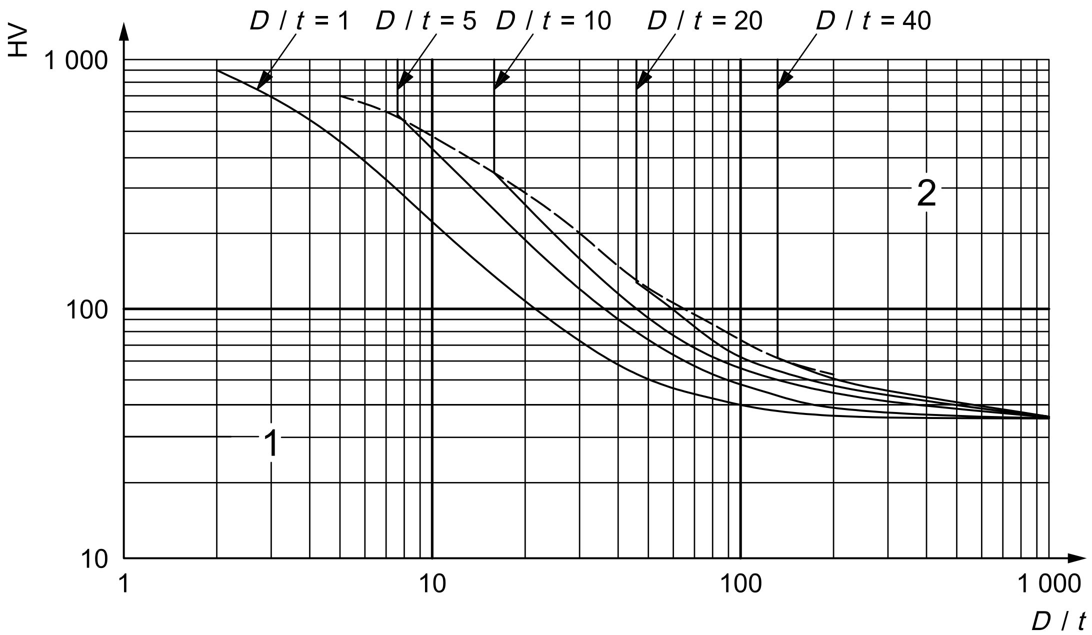

Key

D initial particle diameter

HV Vickers hardness

t film (shim) thickness

1 safe

2 unsafe

Figure 13 — Relationship of the Vickers hardness of particles to the ratio of the initial particle diameter and oil film thickness

In Figure 13, D and t indicate the form of the particles, where t is thickness and D flattish extension. The figure shows safe and unsafe areas for particles of different size and Vickers hardness.

Figure 13 indicates the predicted lines of safe and unsafe particle aspect ratios prior to squashing between cobalt steel anvils with a separating film. The straight lines above the dotted line represent those particles which can just be elastically enclosed by the anvils but whose hardnesses are sufficiently high that no further extrusion will take place. Particles on the curved lines below the dotted line are further extruded during squashing such that the final shape can just be elastically enclosed by the anvils.

Figure 13 indicates that, in the safe area, no permanent indentation has been created, while the definition of the test implies that the unsafe area contains all sizes of permanent indentations, but clearly small ones are inconsequential to life.

Most dangerous are round particles with $D/t = 1$. The test indicates that the influence of hardness is greatest between 35 HV to 600 HV.

The tests described in Figures 13 and 14 give no safe indication of how tough (not brittle), very hard contamination particles influence the bearing life, but as the depths of indentations formed are dependent on particle hardness, the risk of life reduction rises with increased hardness of the particles, including hardnesses above 600 HV.

Figure 14 indicates aspect ratios D/t of particles of size D, which have been pressed between cobalt steel anvils. A range of shim sizes, t, was used to determine the transition from particles which could be elastically enclosed without damaging the anvil and those which caused plastic indentation. The curves represent the transition predicted by a rigid anvil analysis (line 2) and an elastic anvil analysis (line 1).

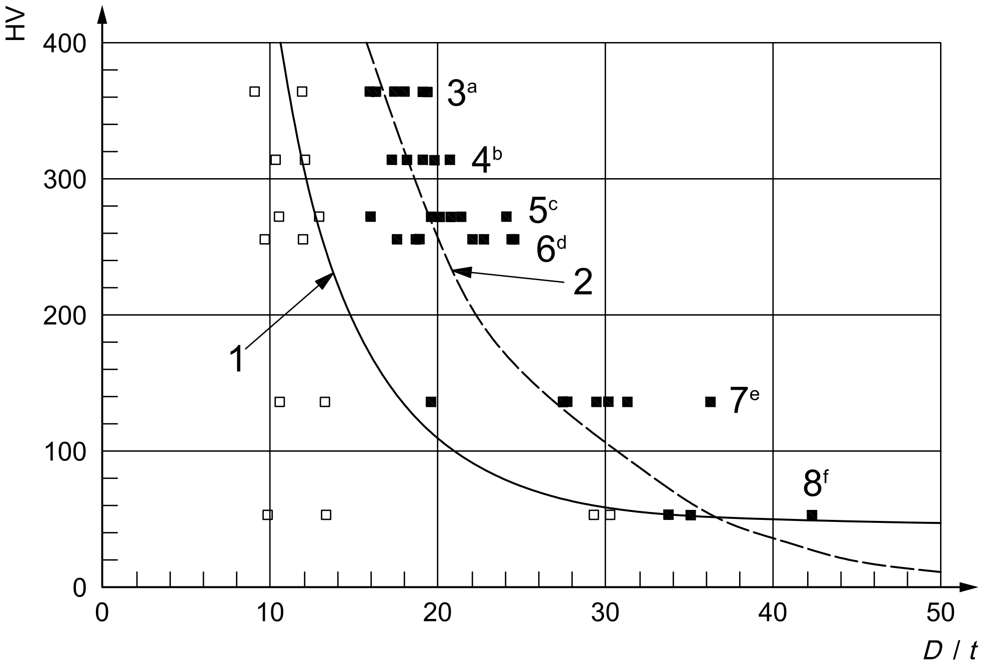

Key

D initial particle diameter
HV Vickers hardness
t film (shim) thickness
1 elastic analysis with friction
2 rigid anvils with friction
□ elastically enclosable particles causing no damage to the anvil
■ particles causing plastic indentation

a Silver steel.
b Welding rod.
c Soft steel.
d Brass.
e Copper.
f Aluminium.

Figure 14 — Damaging Vickers hardness of particles as a function of particle size, D, and distance, t, between pressing cobalt steel anvils

5.6.5.5 Evaluation of the contamination factor graphs in ISO 281

The same procedure, which was used in the evaluation of $[\tilde{A}_{m}(\kappa)/\tilde{A}_{0}]^{3/2c}$ in 5.6.3 according to Reference [9], has been used for the asperities and dents contact analysis when evaluating the $\Omega_{rgh}(\kappa)$ and $\Omega_{dnt}(D_{pw}, \beta_{cc})$ functions.

The final derivation of the functional form of the equation in Figure 11 was performed using direct curve-fitted equations of the results of the rolling bearing contact analysis of the functions $[\tilde{A}(\kappa)/\tilde{A}_{0}]^{3/2c}$, $\Omega_{rgh}(\kappa)$, and $\Omega_{dnt}(D_{pw}, \beta_{cc})$.

In the roughness contact calculations in Reference [9], detailed information is given about the real contact area, the maximum shear stress amplitude beneath asperities and number of contact spots. Furthermore, the calculation was performed for different values of the separation of the rolling contact surfaces. Note that in the contamination factor, e_{C}, curves in ISO 281, an upper limit is introduced following additional safety criteria suggested by engineering practice.

The analytic evaluation of the e_{C} factor is still at an initial stage. Thus, it was developed mainly on an empirical basis supported by laboratory tests and application engineering field experience.

5.7 Difference between the life modification factors in Reference [5] and ISO 281

In Reference [5], a_{SLF} as a function of κ is determined for three ranges of the κ values with slight discontinuities where the ranges meet. As only graphs are shown in Reference [5], this is no problem. However, in ISO 281, equations for a_{ISO} are also given, and the equations are very slightly modified in order to avoid any discontinuities in the equations. The very small difference between calculated a_{SLF} and a_{ISO} is negligible.

6 Background to the ranges of ISO 4406[3] cleanliness codes used in ISO 281, Clauses A.4 and A.5

6.1 General

In ISO 281:2007, Annex A, the estimation of the factor e_C is based on the lubricating oil cleanliness under different operating conditions. The ISO 4406[3] contamination code for 5 µm [or 6 µm(c)] and 15 µm [or 14 µm(c)] particle sizes is used for determining the cleanliness of the oil. The quantities of 5 µm [or 6 µm(c)] and 15 µm [or 14 µm(c)] particles counted are plotted on a graph and connected with a line, which is extended to a probable maximum particle size (see Figures 15 and 16). For such lines, each basic ISO 4406[3] code level is shown by a large dot at 5 µm, 15 µm and at the end of the lines. For each basic level, graphs and equations for estimating the contamination factor, e_C, can be found in ISO 281:2007, Annex A.

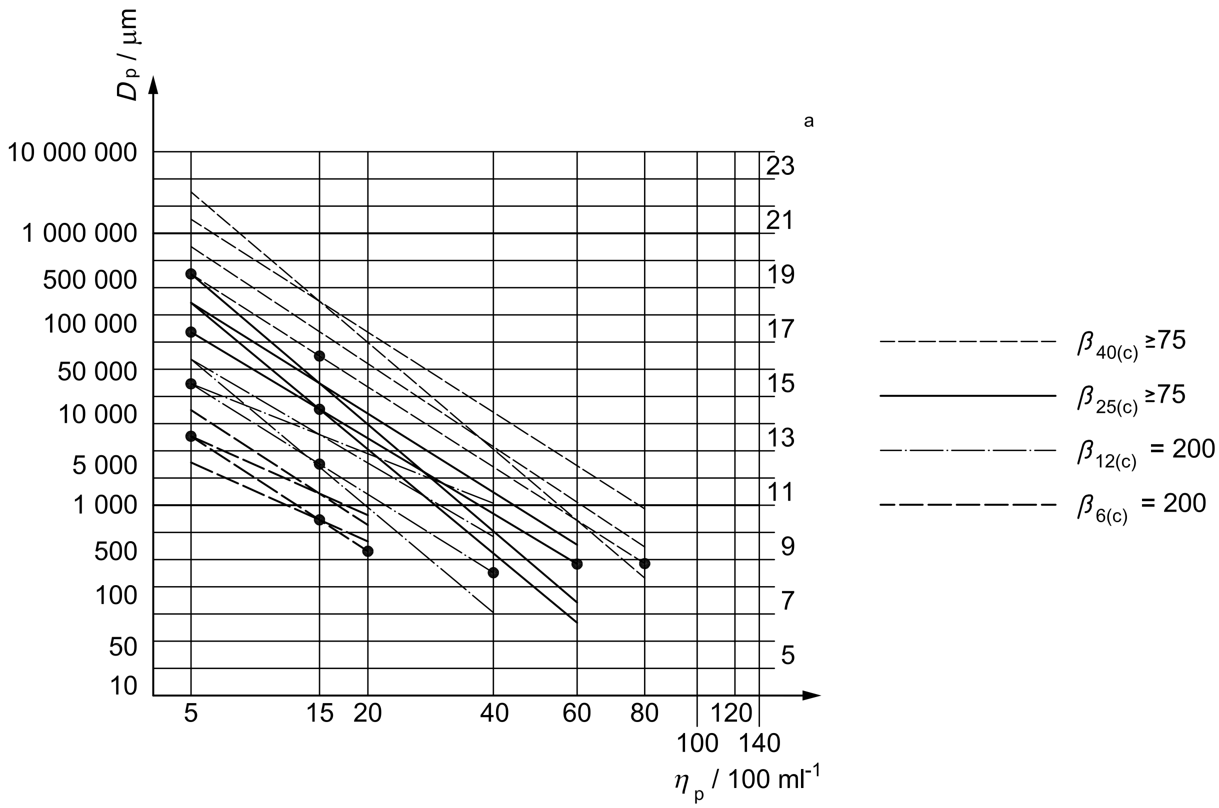

Key

D_p particle size

n_p particle density

● basic codes

a Code.

Figure 15 — On-line filtered oil

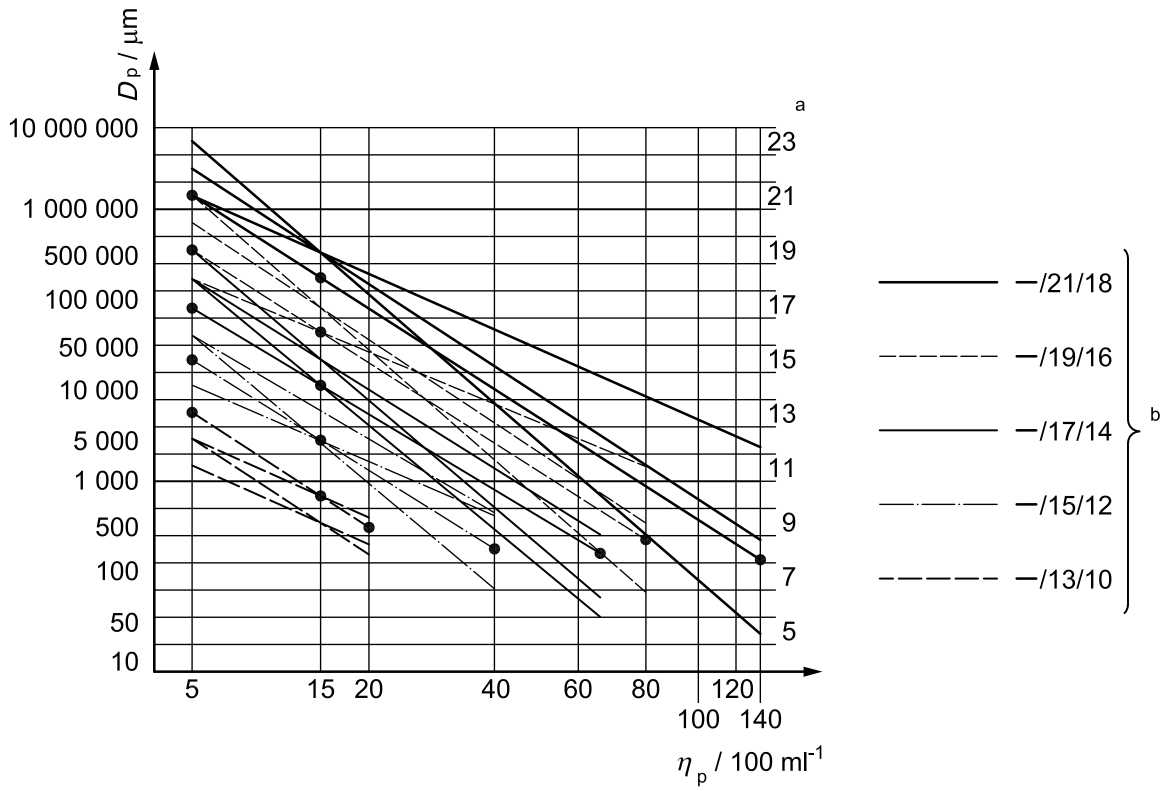

Key

D_p particle size

n_p particle density

● basic codes

a Code.

b Code according to ISO 4406.

Figure 16 — Oil bath

The reason for extended lines is that, in ISO 4406[3], the measurement is based on particles smaller than 15 µm, and, for rolling bearings, such small particles primarily have influence on bearing fatigue life only for small bearings. Large numbers of small particles mainly cause wear of the raceways and rolling elements.

Bearing failures caused by raceway fatigue, e.g. by spalling on the raceway surfaces, is mainly caused by particles larger than 15 µm, and the theory behind the life modification factor, a_{ISO}, is among other things based on the size and quantity of large hard particles.

Therefore, the lines in the graphs are extended and the basic lines provided with three large dots. The large dots at the end of the extended lines represent particles of certain sizes and quantities which have been established by laboratory tests and results from different practical applications. Particle counts have been made for circulated oil-lubricated applications with on-line filters with different filtration ratios and oil bath-lubricated applications, and especially the quantity of large particles for different lubricating conditions have been specially studied.

As the results from particle counts of oil samples from bearings in operation cannot be expected to follow one of the basic lines exactly, each basic line has been given an acceptable range illustrated by surrounding lines.

Each basic code level is defined by a code designation, e.g. —/13/10, where 13 represents the quantity of counted 5 µm [or 6 µm(c)] particles and 10 the quantity of counted 15 µm [or 14 µm(c)] particles, according to ISO 4406[3].

For on-line filtration, the probable maximum particle size for a different filtration ratio $\beta_{x(c)}$ can be estimated with fairly good accuracy. For oil bath lubrication, the estimation is less accurate, as larger particles than indicated in Figure 15 can also be expected, and this is therefore compensated for by an uncertainty factor.

6.2 On-line filtered oil

For on-line filtered oils, the basic ISO 4406[3] code levels and their proposed ranges are illustrated in Figure 15 for different filtration ratios, $\beta_{x(c)}$.

With the aid of Figure 15, basic ISO 4406:1999[3] codes and their ranges are proposed in Table 2 for the different filtration ratios.

Table 2 — Proposed basic ISO 4406:1999[3] codes and their ranges for different filtration ratios

Filtration ratio at contamination particle size x $\beta_{x(c)}$	ISO 4406:1999 code	ISO 4406:1999 code ranges
$\beta_{6(c)} = 200$	—/13/10	—/12/10, —/13/11, —/14/11
$\beta_{12(c)} = 200$	—/15/12	—/16/12, —/15/13, —/16/13
$\beta_{25(c)} \geqslant 75$	—/17/14	—/18/14, —/18/15, —/19/15
$\beta_{40(c)} \geqslant 75$	—/19/16	—/20/17, —/21/18, —/22/18

6.3 Oil bath

For an oil bath, the basic ISO 4406[3] code levels and their proposed ranges are illustrated in Figure 16. The ranges are slightly more restricted for oil bath lubrication. The fact that large particles can be expected in oil bath lubrication is, however, primarily accounted for by the uncertainty factor, s (see 5.6.5.2).

With the aid of Figure 16, basic ISO 4406:1999[3] codes and their ranges are proposed in Table 3.

Table 3 — Proposed basic ISO 4406:1999[3] codes and their ranges (oil bath)

ISO 4406:1999 code	ISO 4406:1999 code ranges
—/13/10	—/12/10, —/11/9, —/12/9
—/15/12	—/14/12, —/16/12, —/16/13
—/17/14	—/18/14, —/18/15, —/19/15
—/19/16	—/18/16, —/20/17, —/21/17
—/21/18	—/21/19, —/22/19, —/23/19

6.4 Contamination factor for oil mist lubrication

Oil mist lubrication is not dealt with as a separate lubrication method in ISO 281.

For oil mist lubrication, ISO 281:2007, 9.3.3.2, is also valid and general guideline values for the contamination factor, e_C, can be selected from ISO 281:2007, Table 13, in the same way as for other lubrication methods. ISO 281:2007, Table 13, shows typical levels of contamination for well-lubricated bearings.

Using more information for the level of cleanliness, accurate and detailed guide values of e_C for oil mist lubrication could be obtained by means of the graphs and equations in ISO 281:2007, Clause A.6, which provides e_C values which are based on grease lubrication.

Selection of graphs and equations for estimating e_C for oil mist lubrication can be made by means of ISO 281:2007, Table A.1, and the conditions for oil mist lubrication of the bearing application estimated by comparison with the operating conditions for grease lubrication. Other factors, such as cleanliness of the assembly, environment and seals, oil-bath or no oil bath, have then to be considered.

7 Influence of wear

7.1 General definition

Wear is the progressive removal of material resulting from the interaction of two sliding or rolling/sliding contacting surfaces during service.

Theoretical estimation of time to failure because of wear is very complex and incomplete. In the following some general information about wear in bearings is given and its influence on bearing operation is discussed.

7.2 Abrasive wear

Abrasive wear is the result of material being cut away from the raceways either by contacting surface asperities due to inadequate lubrication or by the ingress of foreign particles. During a continuing wearing process, the surfaces become dull to a degree, which varies according to the coarseness and nature of the abrasive particles. These particles gradually increase in number as material is worn away from the running surfaces and the cage. Finally, the wear may become an accelerating process that results in a failed bearing. If, however, the wear ceases, after a “mild running-in”, the effect on bearing life need not be negative.

7.3 Mild wear

Sometimes operation with a small κ value, far below 1, has to be accepted, e.g. due to very slow rotational speed and/or high operating temperature. With a good lubricant, with proper additives to prevent smearing, the operating conditions can be much improved when, during the “running-in” period, smoothing of the contacting surfaces takes place. The raceways get a reduced size of surface irregularities and hence an increased real κ value. A rather clean operating condition is required to improve the κ value. Without the presence of foreign particles, surfaces can attain a shiny, mirror-like appearance.

The bearing life can be much increased in relation to the life indicated by the original κ value and, after “running-in”, the operating temperature stabilizes or is even reduced. This may also apply to the noise level.

7.4 Influence of wear on fatigue life

The contact conditions between rolling element and raceways is changed by wear. The conformity between rolling elements and raceways after production is determined such that best possible contact conditions are obtained. For roller contacts, it is important to avoid edge stress during operation.

By wear, full conformity, i.e. line contact under zero load, can be obtained and hence edge loading produced in the roller contacts during operation. Even if the wear itself may be too small to cause a bearing failure, this edge loading can considerably reduce the fatigue life of the bearing.

A special kind of edge loading, caused by wear, occurs in a curved roller/raceway contact, e.g. in spherical roller bearings (see Figure 17). In a curved contact, localized sliding occurs in opposite directions during rotation (see Figure 18). In the position where the sliding changes direction, only rolling and no sliding occurs (see rolling points indicated in Figure 17). In the presence of abrasive particles, wear will take place in the sliding parts of the contacts and no wear in the non-sliding positions. The result is a wavy formed contact with, in the case of spherical roller bearings, two peaks in the position where no sliding occurs. During operation, high contact stress in the peak contacts often results in flaking and early fatigue failure.

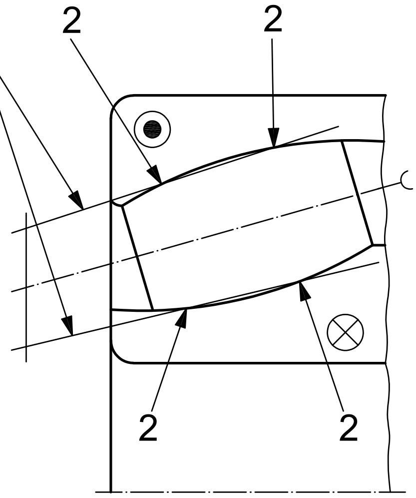

Key

1 rolling cones

2 rolling points

Figure 17 — Contacting conditions in a curved contact

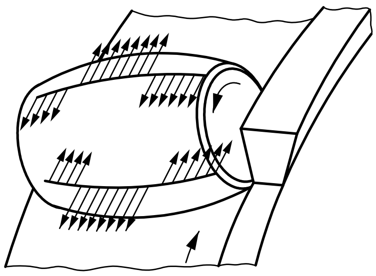

Figure 18 — Sliding in a curved contact

7.5 Wear with little influence on fatigue life

Surface fatigue of the type shown in 7.4 occurs mainly when the wear rate is slow — not aggressive or due to a small quantity of abrasive particles.

In cases where the wear rate is such that peaks are worn away before they are built up, surface fatigue failures normally do not occur. The bearings fail for other reasons. For large bearings running at slow speeds, too large a radial internal clearance due to wear can for instance be the reason for a bearing replacement, often after the bearing has been in operation successfully for a long period of time.

7.6 Adhesive wear

Adhesive wear is a transfer of material from one surface to another with frictional heating and, sometimes, tempering or rehardening of the surface. This produces localized stress concentrations with the potential for cracking or flaking of the contact areas.

Smearing (skidding) can occur between rolling elements and raceways due to the fact that the rolling elements are lightly loaded and subjected to severe acceleration on their re-entry into the load zone (see Figure 19). To prevent smearing, increased lubricant viscosity and/or extreme pressure (EP) additives in the lubricant usually help. Oil is generally better than grease to prevent this kind of smearing. Smearing can also occur between rolling elements and raceways when the load is too light in relation to the speed of rotation.

Smearing can occur on the guiding flange faces and on the ends of the rollers due to insufficient lubrication (see Figure 20). In full complement bearings (cageless), smearing can also occur in the contacts between rolling elements depending on lubrication and rotation conditions. Increased lubricant viscosity and/or EP additives in the lubricant are also recommended in this case.

If a bearing ring "rotates" relative to its seating, i.e. mounting shaft or housing, then smearing can occur in the contact between the ring end face and its axial abutment, which can also cause cracking of the ring as shown in Figure 21. This type of damage generally occurs when the radial load on the bearing rotates relative to the bearing ring and the bearing ring is mounted with a small clearance (loose fit) to its seating. Because of the minute difference in the diameters of the two components, they have a minute difference in their circumferences and, consequently, when brought into contact at one point by the radial load, rotate at minutely different speeds. This rolling motion of the ring against its seating with a minute difference in the rotational speeds is termed "creep". If a tighter fit, without clearance during operation, can be accepted, that normally solves the problem.

When creep occurs, the asperities in the ring/seating contact region are over-rolled, which can cause the surface of the ring to take on a shiny appearance. The over-rolling during creeping is often, but not necessarily, accompanied by sliding in the ring/seating contact, and then other damage will also be visible, e.g. scratches, fretting corrosion and wear. Under certain loading conditions and when the ring/seating interference fit is insufficiently tight, then fretting corrosion will predominate.

Figures 19 to 21 are reproduced from ISO 15243[4].

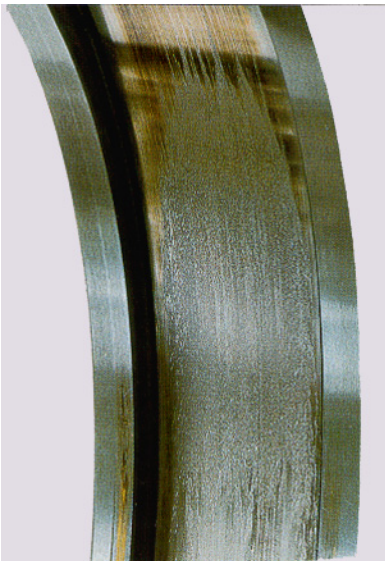

Figure 19 — Smearing on raceway surfaces

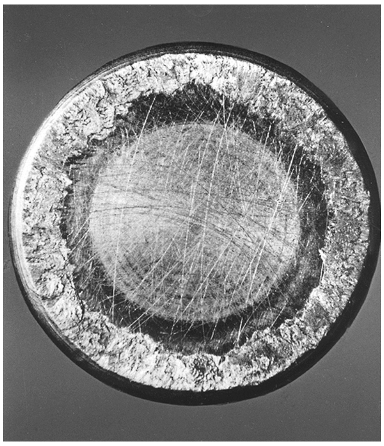

Figure 20 — Smearing on roller end

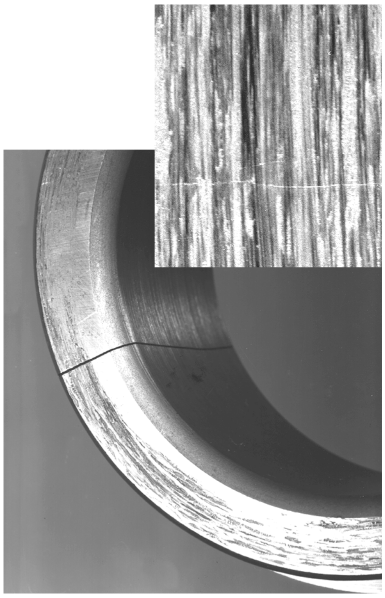

Figure 21 — Smearing on ring end face (ring also fractured)

8 Influence of a corrosive environment on rolling bearing life

8.1 General

The service life of rolling bearings is reduced by operation in a corrosive environment and sometimes to an extremely high degree. Despite the fact that considerable knowledge about influence of corrosive environments exists, there are few data available for estimating the effect on bearing life. Documented results from tests also show great variation.

8.2 Life reduction by hydrogen

8.2.1 Hydrogen atom penetration

Research indicates that in a corrosive environment the main factor for life reduction is presence of hydrogen atoms.

Water content in the lubricant has deleterious effects on the endurance life of bearings. This water is dissolved into the lubricating oil during operation of rolling bearings. Interactions of water and bearing steel surfaces under applied stresses give rise to hydrogen generation and to hydrogen embrittlement failure.

The Hertzian stresses in the contact zone are principally compressive in nature but are tensile at the periphery. The hydrogen is known to be attracted to the core of dislocation under the action of tensile stress. This hydrogen will arrest the dislocation during repeated stress cycles and thus results in stepwise void coalescence and early failure of the raceways of rolling bearings.

The influence of life reduction by hydrogen is dealt with more extensively in Reference [11].

8.2.2 Hydrogen atoms derived from raceway contacts

8.2.2.1 General

From liquids containing hydrogen in the lubricant, e.g. water and acids and from the lubricant itself, hydrogen atoms can be separated by chemical and galvanic processes in the rolling element/raceway contacts. The hydrogen atoms penetrate the bearing steel and some of them hit particle inclusions.

The hydrogen atom separation takes place primarily during rotation. The rolling element raceway contact then prevents the formation of a protective surface layer.

8.2.2.2 Influence of water on bearing life

It is very difficult to establish a general rule regarding the influence of water in the lubricant on bearing life. Results from research show very great dispersion. In Reference [12] the results from some tests are shown.

The bearing lives calculated by means of ISO 281 are valid for the content of water in well protected bearings in practical operation or in tests. The expected content of water as a mass fraction can be 0,02 % to 0,05 %. If possible the lower value should be aimed at.

As a rule of thumb, bearing life is reduced to half its value for each doubling of the water content from 0,02 % mass fraction. On the other hand, the bearing life can be expected to be more than doubled for water content values close to zero. These rules are based on results from lightly loaded bearings. Laboratory tests indicate, however, that the influence of the water content on the life of heavily loaded bearings is much lower.

These figures are only to be regarded as very rough estimations as different oils, greases and additives have different effects on the influence of water in the lubricant.

Water content above 1 % mass fraction may not have so much more influence on the fatigue life, but instead other forms of damage may occur, such as smearing, corrosion, and reduced ability to build up an oil film in the rolling element raceway contact, which may result in a very short service life. To estimate theoretically an expected service life under such conditions is not possible, and the service life then has no connection with the theory behind the calculation of the fatigue life of rolling bearings.

8.2.2.3 Influence of EP additives on bearing life

EP additives in the lubricant are used to improve the lubrication condition when the oil film in the rolling element contacts is thin (small κ value, e.g. when $\kappa < 0{,}5$) and also to prevent smearing between lightly loaded rollers and raceway, e.g. when especially heavy rollers enter a loaded zone with reduced speed.

However, EP additives of the sulfur-phosphorus type, which are most commonly used today, also have a negative influence on the fatigue life of the bearings. This is described in tests reported in Reference [12].

The reason for this negative influence is that in the presence of humidity, which can never be completely avoided, sulfur and phosphorus acids are produced and facilitate the separation of hydrogen atoms in the rolling element contacts during rotation. As described in 8.2.1, the penetration of hydrogen atoms into the steel can considerably reduce the fatigue life of the bearings.

The life reduction increases with temperature and, for temperatures above 90 °C, a lubricant with EP additives should only be used after careful testing.

8.2.3 Hydrogen in bearing steel

Hydrides, consisting of hydrogen atoms and metals, e.g. iron, also exist in the bearing steel, and therefore hydrogen is difficult to eliminate.

In the ingots, the content of hydrides is high, but with the course of time and by rolling and forging processes the content is much reduced. By repeated forging processes, the inclusions become smaller and smaller and the hydride content lowered further and further and the quality of the steel is improved from the fatigue strength point of view.

The hydrogen content of steel for small ball bearings can be as low as $0{,}1 \times 10^{-6}$ mass fraction. For larger bearings, the content can be 2×10^{-6} mass fraction or more.

The hydrogen inclusions have a negative influence on bearing life which is added to the influence of the raceway surface-originated hydrogen atoms described in 8.2.1.

8.2.4 Conclusion

Hydrogen atoms in the lubricant and in the steel contribute to reduce the fatigue strength of the bearing steel. The fatigue stress limit used for calculating the dynamic load ratings can be considerably reduced thereby due to the concentration of hydrogen atoms around particle inclusions. Especially sensitive are the volumes subjected to tensile stress.

In order to avoid reduction of the fatigue stress limit, the water content in the lubricant should be as small as possible and EP additives, if used, have to be carefully selected and adapted to the operating temperature. When specifying the requirement for bearing steel, it is important to have in mind not only the cleanliness of the steel but also the importance of efficient rolling and forging processes.

8.3 Corrosion

8.3.1 General definition

Corrosion is a chemical reaction on metal surfaces.

8.3.2 Moisture corrosion

When steel, used for rolling bearing components, is in contact with moisture, e.g. water or acid, oxidation of surfaces takes place. Subsequently, the formation of corrosion pits occurs and, finally, flaking of the surface (see Figure 22). Cracked inner rings sometimes occur, where the cracks originate from pits. The risk of cracking increases where brittleness is caused by presence of hydrogen atoms as described in 8.2

A specific form of moisture corrosion can be observed in the contact areas between rolling elements and bearing rings where the water content in the lubricant or the degraded lubricant reacts with the surfaces of the adjacent bearing elements. The advanced stage will result in dark discolouration of the contact areas at intervals corresponding to the ball/roller pitch, eventually producing corrosion pits (see Figures 23 and 24).

Moisture corrosion, often in combination with surface fatigue, e.g. in the form of flaking, can cause short service life of a bearing. Estimating service life or fatigue life by calculation is of course not possible. The application of the bearings has to be made such that ingress of moisture is prevented.

Figures 22 to 27 are reproduced from photos in ISO 15243[4].

Figure 22 — Corrosion on roller bearing outer ring

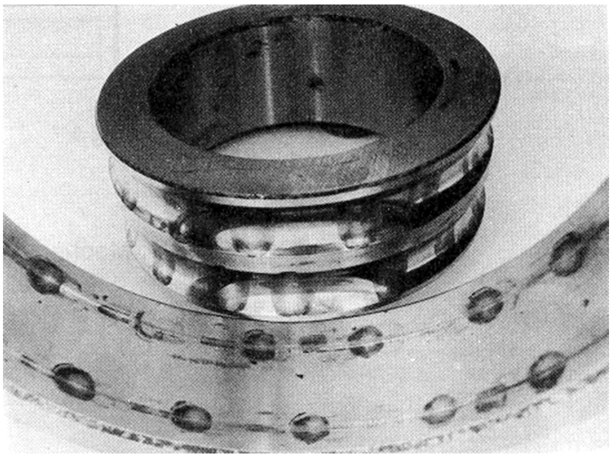

Figure 23 — Contact corrosion on a ball bearing inner ring and outer ring raceway

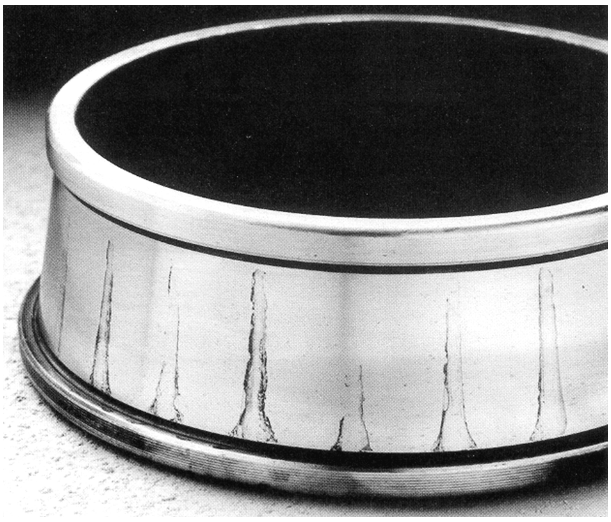

Figure 24 — Contact corrosion on a bearing raceway

8.3.3 Frictional corrosion

8.3.3.1 General definition

Frictional corrosion is a chemical reaction activated by relative micromovements between mating surfaces under certain friction conditions. These micromovements lead to oxidation of the surfaces and material becoming visible as powdery rust and/or loss of material from one or both mating surfaces.

8.3.3.2 Fretting corrosion

Fretting corrosion occurs in fit interfaces that are transmitting loads under oscillating contact surface micromovements. Surface asperities oxidize and are rubbed off and vice versa; powdery rust develops (iron oxide). The bearing surface becomes a shiny or discoloured blackish red (see Figure 25). Typically, the failure develops in incorrect fits, either too light an interference fit or too high a surface roughness, in combination with loads and/or vibrations.

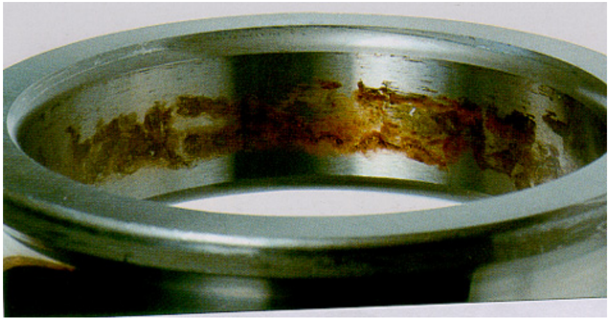

Figure 25 — Fretting corrosion in inner ring bore

8.3.3.3 False brinelling

False brinelling occurs in rolling element/raceway contact areas due to micromovements and/or resilience of the elastic contacts under cyclic vibrations. Depending on the intensity of the vibrations, the lubrication conditions and load, a combination of corrosion and wear occurs, forming shallow depressions in the raceways.

In the case of a stationary bearing, the depressions appear at rolling element pitch and can often be discoloured, reddish or shiny (see Figure 26).

False brinelling caused by vibrations occurring during rotation shows itself in closely spaced flutes (see Figure 27). These should be distinguished from electrically caused flutes. The fluting resulting from vibration has bright or fretted bottoms to the depressions compared to fluting produced by the passage of electric current, where the bottoms of the depressions are dark in colour. The damage caused by electric current is also distinguishable by the fact that the rolling elements are also marked.

NOTE In this document, false brinelling is classified under corrosion. In other documents, it is sometimes classified as wear.

One problem with false brinelling is vibration and noise, which often requires that the bearings be replaced before the depressions cause early surface fatigue.

To prevent false brinelling, the bearing application has to be made such that the micromovements are avoided, e.g. by axial preloading of bearings, permanent or only during transportation. In some applications bearings sensitive to micromovements are replaced by less sensitive bearings. Cylindrical roller bearings are, for instance, replaced by ball bearings in applications where axial micromovements can be expected.

Figure 26 — False brinelling on inner ring raceway of cylindrical roller bearing

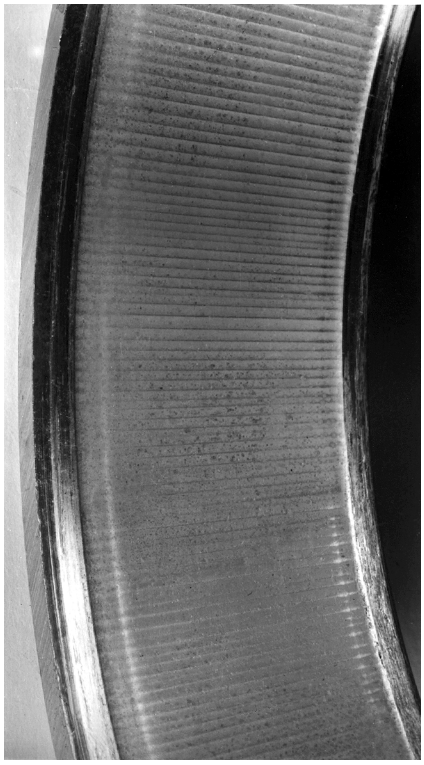

Figure 27 — False brinelling — Fluting on outer ring of tapered roller bearing

9 Fatigue load limit of a complete rolling bearing

9.1 Influence of bearing size

In the equations for C_u in ISO 281:2007, B.3.2.2 and B.3.3, the reduction factors $(100/D_{pw})^{0,5}$ for ball bearings and $(100/D_{pw})^{0,3}$ for roller bearings are used for the pitch diameter $D_{pw} > 100$ mm.

The reduction factors are primarily based on the fact that the fatigue stress limit is reduced for large size bearings. Among other things, this is for large dimensions caused by less effective kneading of the ingots during the rolling and forging operations.

For high quality bearing steel, the fatigue limit can be obtained for a contact stress of 1 500 MPa for bearings with pitch diameters up to 100 mm. Fatigue tests of steel, used for bearings with a pitch diameter of 500 mm, have shown that the fatigue stress limit can be obtained for a contact stress of 1 100 MPa (see Reference [12], section 2.2.3).

With 1 100/1 500 = 0,73, a reduction of 70 % to 80 % of the fatigue load limit for bearings with pitch diameters of 500 mm can be expected. This has been considered by adding the above-mentioned reduction factors $(100/D_{pw})^{0,5}$ for ball bearings and $(100/D_{pw})^{0,3}$ for roller bearings for $D_{pw} > 100$ mm in the equations for calculating the fatigue load limit. The factors $(100/D_{pw})$ and their exponents are determined by practical engineering estimation, bearing the reduction of the fatigue limit for large dimension bearings in mind.

Figures 28 and 29 are based on the maximum shear stresses below the rolling element contacts, caused by the calculated load, C_u, when the size of this fatigue load is calculated by means of the simplified equations in ISO 281:2007, B.3.3. Calculations have been carried out for different sizes of two bearing types.

The curves show the maximum contact shear stress caused by the calculated (by means of the simplified equations) load, C_u, for a bearing with a certain pitch diameter, D_{pw}, divided by the corresponding shear stress for a bearing with 100 mm pitch diameter.

The contact stress has also been calculated under the same loading conditions as the shear stress, and the result gives almost exactly the same maximum contact variation as a function of the pitch diameter. The shear stress curves therefore also represent the contact stress relationship.

The graphs confirm that the shear stress level is well accounted for and reduced with bearing size. For a pitch diameter of 500 mm, the reduction is 70 % to 80% for the bearings shown.

The graphs thus confirm that the reduction factors $(100/D_{pw})^{0,5}$ for ball bearings and $(100/D_{pw})^{0,3}$ for roller bearings determined by a practical engineering approach, based on fatigue stress reduction for large dimensions, give a reliable result.

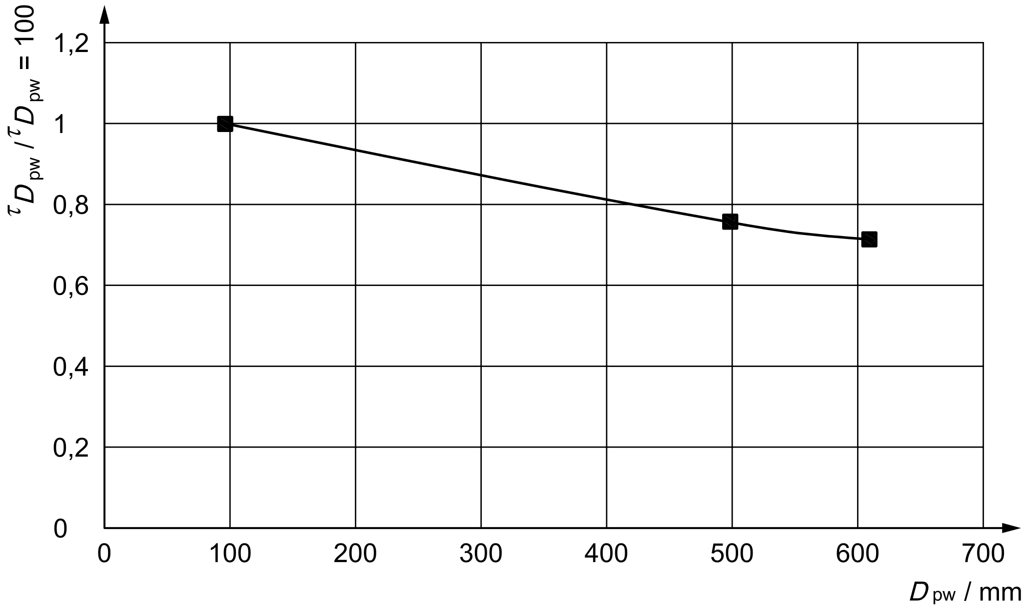

Key

D_{pw} pitch diameter

$\tau_{D_{pw}}$ shear stress for D_{pw}

$\tau_{D_{pw}} = 100$ shear stress for $D_{pw} = 100$

Figure 28 — Maximum shear stress variation as a function of pitch diameter for deep groove ball bearings

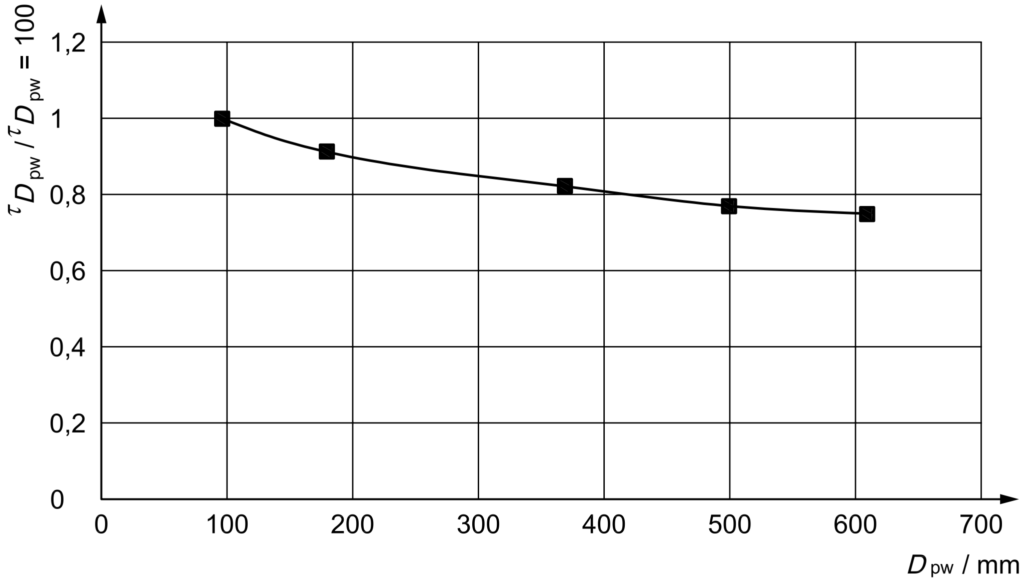

Key

D_{pw} pitch diameter

$\tau_{D_{pw}}$ shear stress for D_{pw}

$\tau_{D_{pw} = 100}$ shear stress for $D_{pw} = 100$

Figure 29 — Maximum shear stress variation as a function of pitch diameter for cylindrical roller bearings

9.2 Relationship fatigue load limit divided by basic static load rating for calculating the fatigue load limit for roller bearings

In the equations of ISO 281:2007, B.3.3.3, for simplified calculation of C_u for roller bearings, the relationship $C_u = C_0/8,2$ is used. The background to the value 8,2 in this relationship is here explained.

From the roller bearings literature (e.g. Reference [18]), it is known that, when the bearing clearance is zero, the bearing radial load, F_r, in newtons, is given by

$$F_r = 0{,}245\,3\ Q_{max}\, Z \cos\alpha \tag{29}$$

where

Q_{max} is the maximum load, in newtons, of a single contact;

Z is the maximum number of rolling elements per row;

α is the nominal contact angle, in degrees.

For normal bearing clearance in operation, Equation (30) is often used

$$F_r = 0{,}2 Q_{max}\, Z \cos\alpha \tag{30}$$

For this clearance, the loaded zone extends to around 130°.

Insert $F_r = C_0$ and $Q_{max} = Q_0$ in Equation (30) due to the fact that C_0 is based on bearings with normal clearance in operation. Also, insert $F_r = C_u$ and $Q_{max} = Q_u$ in Equation (29) due to the fact that C_u is based on bearings with zero clearance. Equation (31) can then be derived:

$$\frac{C_0}{C_u} = \frac{Q_0}{Q_u} \frac{0{,}2}{0{,}245\,3} \tag{31}$$

From the roller bearings literature, e.g. Reference [18], it is known that for line contact, $Q \approx p^2$, where p is the pressure in the roller/raceway contact, hence:

For C_0, the maximum contact stress is $p = 4\ 000$ MPa according to ISO 76[1].

For C_u, the maximum contact stress is $p = 1\ 500$ MPa according to ISO 281:2007, 9.3.1.

Equation (31) can then be written

$$\frac{C_0}{C_u} = \left(\frac{4\ 000}{1\ 500}\right)^2 \frac{0{,}2}{0{,}245\ 3} \tag{32}$$

The maximum stress, 1 500 MPa, is obtained for a mean Hertzian stress of around 1 250 MPa (see Figure 30), where the contact stress is shown as a function of the contact length, x, expressed in relation to the effective roller length, L_{we}, as $2x/L_{we}$. By relating C_u to this value, Equation (32) can be written

$$\frac{C_0}{C_u} = \left(\frac{4\ 000}{1\ 500}\right)^2 \frac{0{,}2}{0{,}245\ 3} \left(\frac{1\ 500}{1\ 250}\right)^2 = 8{,}31 \tag{33}$$

Depending on the contacting conditions, the actual range for C_0/C_u is 7,2 to 9,5, and a typical value is 8,2, to which Equation (33) yields a close approximation.

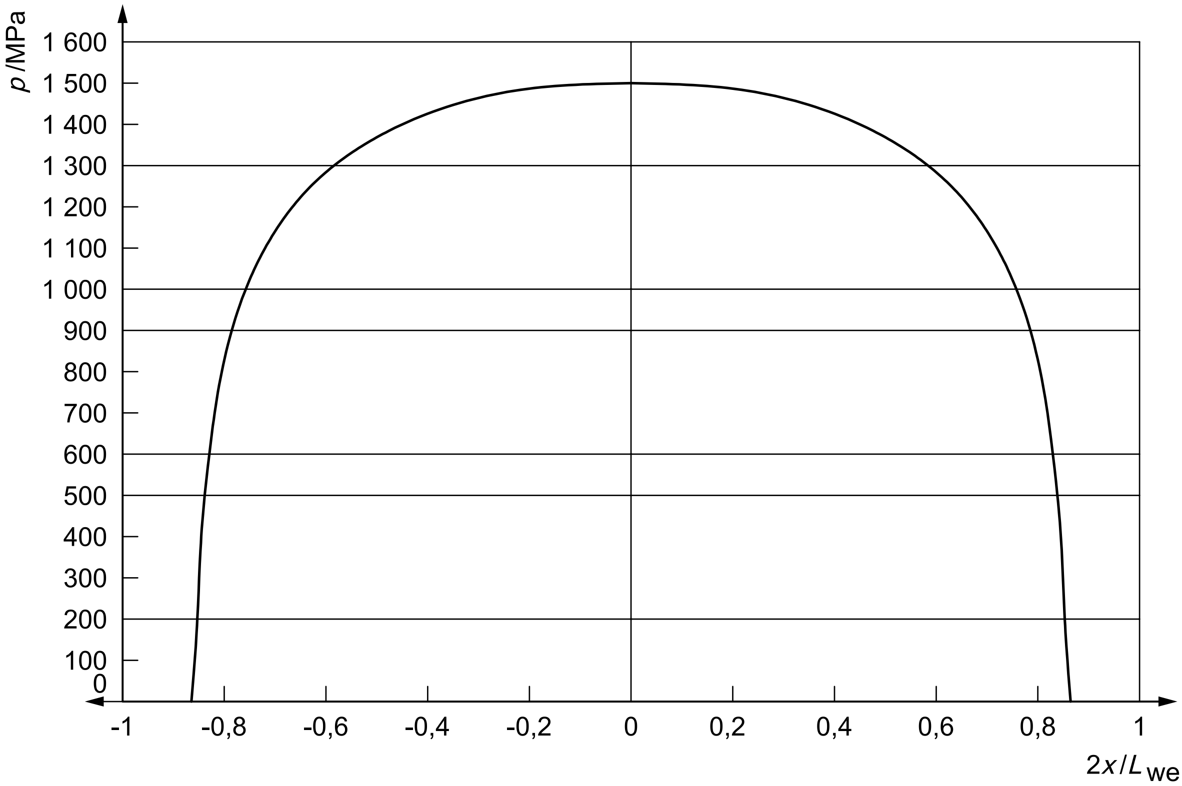

Key

L_{we} effective roller length

p contact stress for a load, $P = C_u$

x contact length

NOTE Hertzian contact stress: 1 250 MPa; actual contact stress: 1 500 MPa.

Figure 30 — Contact stress distribution when the roller bearing is subjected to a load corresponding to the basic static radial load rating

10 Influence of hoop stress, temperature and particle hardness on bearing life

10.1 Hoop stress

In bearing applications, different levels of interference are required to prevent ring rotation relative to the shaft or the housing, and thus prevent fretting. This interference depends primarily on the magnitude of applied loading and secondarily on the shaft speed. The greater the applied load and shaft speed, the greater must be the interference to prevent ring rotation. In most cases, this interference causes tensile stresses in the inner rings of the bearings, i.e. hoop stresses, which are known to reduce the fatigue life of rolling bearings (References [12], [13], and [14]). Hoop stresses can also result from the high speed rotation of a ring. At the same time, additional internal stress fields exist in the bearing rings (and rolling elements), the residual stress fields, that are created during the manufacturing of the rings. These stresses can substantially change during the operation of the bearing (Reference [15]). The residual stresses are usually larger in magnitude than the hoop stresses, vary with depth from the surface of the ring, and can be compressive or tensile.

Both these additional stresses added together constitute the internal stress field. These internal stresses (press fitting and/or high speed ring rotation, residual stresses) are superimposed on the subsurface stress field caused by contact surface stresses to determine the fatigue life of the bearings. The variation of the internal stresses with the operating conditions of the bearings over time is a current topic of research, but at the time of publication the level of understanding is not sufficient for their quantitative introduction into the standardized bearing life ratings.

10.2 Temperature

Heat treatment of bearing components results in non-stable steel that incurs microstructural alterations under alternating contact stress fields. The level of such alterations depends not only on the alloy composition of the steel and its heat treatment but also on the operating load and temperature (Reference [15]). These microstructural alterations include the transformation of the retained austenite, the evolution of residual stresses and texture, as well as the development of low and high angle bands with local hardness variations. Clearly all these transformations, which depend on the operating temperature of the rings, influence the fatigue life of the rings, but, as previously stated, at the time of publication the level of understanding is not sufficient for the quantitative introduction of the effects of temperature into the standardized bearing life ratings.

10.3 Hardness of contaminant particles

The damage generated by particulate contamination contained in the lubricant on the surfaces of the bearing rings and the rolling elements, and the subsequent bearing life reductions, has been established in many publications. It is clear that, for metallic particles, the size, shape and hardness (see Reference [16]) are the important particle attributes that, together with the bearing size and the bearing operational parameters, define the bearing life reduction (the a_{ISO} life factor or the contamination factor, e_{C}).

In the case of friable (e.g. brittle, ceramic) particles, the important parameters are the particle size and the fracture toughness of its material (Reference [17]). These parameters determine the proximity to the EHL contact of the actual particle fracture, the size of the particle fragments and the resulting damage (dent).

For standardized calculations, there is usually limited knowledge of the particle parameters indicated above and, thus, the e_{C} graphs in both Reference [5] and ISO 281 are plotted for a particle hardness typical of hardened steel, 700 HV. Therefore, this provides a conservative approach to the effects of contamination in graphs for general operating conditions.

If the lubricant contains tough (non-brittle) particles with hardness above 700 HV, the hard particles may reduce the modified rating life calculated according to ISO 281.

11 Relationship between κ and Λ

11.1 The viscosity ratio, κ

If an adequate lubricant film between rolling elements and raceways is to be formed, the lubricant must have a given minimum viscosity when the bearing application has reached its normal operating temperature. The condition of the lubricant is described by the viscosity ratio, κ, for adequate lubrication:

$$\kappa = \frac{\nu}{\nu_1} \tag{34}$$

where

ν is the actual kinematic viscosity;

ν_1 is the reference kinematic viscosity.

The reference viscosity, ν_1, takes acccount of the minimum oil film thickness, h_{min}, needed, in relation to the contacting surface irregularities, to give adequate lubrication. If a lubricant with a higher viscosity at the operating temperature is selected, then a thicker oil film is formed, which, by increased separation of the contacting surfaces, provides improved lubrication conditions and hence an improved bearing life.

11.2 The ratio of oil film thickness to composite surface roughness, Λ

The influence of the oil film thickness on the bearing life can also be dealt with by means of the factor Λ:

$$\Lambda = \frac{h}{s} \tag{35}$$

where

h is the oil film thickness;

s is the root mean square surface roughness, given by

$$s = \sqrt{s_1^2 + s_2^2} \tag{36}$$

in which

s_1 is the surface roughness of contacting body 1,

s_2 is the surface roughness of contacting body 2.

11.3 Theoretical calculation of Λ

11.3.1 Line contact

Equation (37) is obtained from Reference [19] for calculating minimum oil film thickness

$$H_{min} = \frac{2{,}65\bar{U}^{0{,}7} G^{0{,}54}}{\bar{Q}^{0{,}13}} \tag{37}$$

From this expression, the minimum oil film thickness is derived as

$$h_{\text{min}} = R\,H_{\text{min}} \tag{38}$$

The parameters in the equations are given by

$$\bar{U} = \frac{\eta_{\text{o}} U}{2E' R} \tag{39}$$

$$G = \lambda E' \tag{40}$$

in which

$$E' = \frac{E}{1-\xi^2} \tag{41}$$

$$\bar{Q} = \frac{Q}{l\,E'\,R} \tag{42}$$

where

- E is the modulus of elasticity;
- l is the effective roller contact length;
- Q is the rolling element load;
- R is an equivalent radius used for calculating the speed of rotation, of the set of rolling elements and the cage speed, by multiplying with a bearing ring speed n, i.e. $R\,n$;
- U is the entrance velocity of the oil into the contact;
- η_{o} is the dynamic oil viscosity at atmospheric pressure;
- λ is the pressure coefficient of viscosity;
- ξ is Poisson's ratio.

By means of Equations (38), (39), (40), (41) and (42) is obtained:

$$h_{\text{min}} = \frac{R\;2{,}65\left(\eta_{\text{o}} U / 2E'R\right)^{0{,}7}\left(\lambda E'\right)^{0{,}54}}{\left(Q / lE'R\right)^{0{,}13}} \tag{43}$$

Equations (35), (36) and (43) give the lubrication condition for the viscosity η_{o} expressed by Λ.

$$\Lambda = \frac{h_{\text{min}}}{\sqrt{s_1^2 + s_2^2}} = \frac{R}{\sqrt{s_1^2 + s_2^2}}\;\frac{2{,}65\left(\eta_{\text{o}} U / 2E'R\right)^{0{,}7}\left(\lambda E'\right)^{0{,}54}}{\left(Q / lE'R\right)^{0{,}13}} \equiv a\,\eta_{\text{o}}^{0{,}7}\,\lambda^{0{,}54} \tag{44}$$

The factor λ can, according to Reference [19], be expressed as

$$\lambda = 0{,}112\,2\left(\frac{\nu_{\text{o}}}{10^4}\right)^{0{,}163} \tag{45}$$

where ν_{o} is the kinematic viscosity, in square centimetres per second.

The kinematic viscosity, ν_o, can be derived from

$$\nu_o = \frac{\eta_o}{\rho}$$

where

η_o is the dynamic viscosity;

ρ is the density.

Equation (45) can then be written

$$\lambda \equiv b\eta_o^{0,163} \tag{46}$$

Equation (44) gives

$$\Lambda = a\eta_o{}^{0,7}\lambda^{0,54} = a\eta_o^{0,7}\left(b\eta_o^{0,163}\right)^{0,54} = ab^{0,54}\eta_o^{(0,7+0,163\times 0,54)} = ab^{0,54}\eta_o^{0,788} \tag{47}$$

Then

$$\eta_o = \left(\frac{1}{ab^{0,54}}\right)^{1/0,788}\Lambda^{1,269} \equiv c\Lambda^{1,269} \tag{48}$$

This derivation is made for an oil with a viscosity that gives an adequate lubrication condition, which means a value $\Lambda = \Lambda_1 = 1$. For this special condition, Equation (48) can be written

$$\eta_o = c\Lambda_1^{1,269} \tag{49}$$

For another viscosity, η_o^x, Equation (48) can be written in a general form

$$\eta_o^x = c\Lambda^{1,269} \tag{50}$$

In this case, all conditions are the same except the change of viscosity from η_o to η_o^x, and therefore the factor c is not changed.

Equation (34) can be written

$$\kappa = \frac{\nu}{\nu_1} = \frac{\eta_o^x}{\eta_o} \tag{51}$$

considering that $\nu_o = \eta_o/\rho$ and the fact that the density, ρ, is assumed to be constant.

Equations (49), (50) and (51) give

$$\kappa = \frac{\eta_o^x}{\eta_o} = \frac{\Lambda^{1,269}}{\Lambda_1^{1,269}} = \Lambda^{1,269} \tag{52}$$

as $\Lambda_1 = 1$

11.3.2 Point contact

From Reference [20], Equation (53) for calculating minimum oil film thickness is obtained:

$$H_{\text{min}} = \frac{3{,}63 \bar{U}^{0{,}68} G^{0{,}49} \left(1 - e^{-0{,}68 k}\right)}{\bar{Q}^{0{,}073}} \tag{53}$$

By comparing Equation (44) and Equation (53) and applying Equation (45) is derived:

$$\Lambda \approx \nu_{\text{o}}^{0{,}68} \lambda^{0{,}49} \approx \nu_{\text{o}}^{0{,}68} \left(\nu_{\text{o}}^{0{,}163}\right)^{0{,}49} \approx \nu_{\text{o}}^{[0{,}68+(0{,}49 \times 0{,}163)]} \approx \nu_{\text{o}}^{0{,}76} \tag{54}$$

Equation (38) can be written

$$\nu_{\text{o}} \approx \Lambda^{1{,}316} \tag{55}$$

In the same way as in Equations (48) to (52) can be derived:

$$\kappa = \Lambda^{1{,}316} \tag{56}$$

11.3.3 Result

By comparing Equations (52) and (56) and also other calculations, Equation (57) for the relationship between κ and Λ has been decided for point contact and line contact.

$$\kappa = \Lambda^{1{,}3} \tag{57}$$

Bibliography

[1] ISO 76, *Rolling bearings — Static load ratings*

[2] ISO/TR 1281-1, *Rolling bearings — Explanatory notes on ISO 281 — Part 1: Basic dynamic load rating and basic rating life*

[3] ISO 4406:1999, *Hydraulic fluid power — Fluids — Method for coding the level of contamination by solid particles*

[4] ISO 15243, *Rolling bearings — Damage and failures — Terms, characteristics and causes*

[5] IOANNIDES, E., BERGLING, G., GABELLI, A. *An analytical formulation for the life of rolling bearings.* Finnish Academy of Technology, Helsinki, 1999, 77 p. (*Acta Polytechnica Scandinavica, Mechanical Engineering Series*, Monograph 137.)

[6] TALLIAN, T. Weibull distribution of rolling contact fatigue life and deviations therefrom. *ASLE Trans.* 1962, **5**, p. 183-196

[7] SNARE, B. How reliable are bearings*? Ball Bearing J.* 1970, (162), p. 3-5

[8] TAKATA, H., SUZUKI, S., MAEDA, E. Experimental study of the life adjustment factor for reliability of rolling element bearings. In: *Proceedings of the JSLE International Tribology Conference*, 1985-07-08/10, Tokyo, Japan, p. 603-608. Elsevier, New York, NY, 1986

[9] IOANNIDES, E., KUIJPERS, J.C. Elastic stresses below asperities in lubricated contacts. *J. Tribol.* 1986, **108**, p. 394-402

[10] SADA, T., MIKAMI, T. Effect of lubricant film thickness on ball bearing life under contaminated lubrication: Part 1 — Life tests for ball bearings in contaminated oil. *Jpn. J. Tribol.* 2004, **49**, p. 631-639

[11] SADA, T. and MIKAMI, T. Effect of lubricant film thickness on ball bearing life under contaminated lubrication: Part 2 — Relationship between film thickness and dent formation. *Jpn. J. Tribol.* 2005, **50**, p. 62-67

[12] SADA, T., MIKAMI, T. Effect of lubricant film thickness on ball bearing life under contaminated lubrication: Part 3 — Reciprocal action of contamination and film thickness. *Jpn. J. Tribol.* 2005, **50**, p. 43-49

[13] IMRAN, T. Effect of water contamination on the diffused content of hydrogen under stress in AISI-52100 bearing steel, Doctoral Thesis, Division of Machine Elements, Department of Mechanical Engineering, Lund Institute of Technology, 2005

[14] BARNSBY, R., DUCHOWSKI, J., HARRIS, T., IOANNIDES, E., LOSCHE, T., NIXON, H., WEBSTER, M. *Life ratings for modern rolling bearings — A design guide for the application of International Standard ISO 281/2*, ASME, New York, NY. 90 p. (*TRIB*, Vol 14)

[15] CZYZEWSKI, T. Influence of a tension stress field introduced in the elastohydrodynamic contact zone on rolling contact fatigue. *Wear* 1975, **34**, p. 201-214

[16] IOANNIDES, E., JACOBSSON, B., TRIPP, J. Prediction of rolling bearing life under practical operating conditions. In: DOWSON, D. et al., editors. *Tribological design of machine elements: 15th Leeds-Lyon Symposium on Tribology*, p. 181-187. Elsevier, Amsterdam, 1989

[17] VOSKAMP, A.P. Material response to rolling contact loading. *J. Tribol.* 1985, **107**, p. 359-366

[18] SAYLES, R.S., HAMER, J.C., IOANNIDES, E. The effects of particulate contamination in rolling bearings — A state of the art review. *Proc. Inst. Mech. Eng*. 1990, **204**, p. 29-36

[19] DWYER-JOYCE, R.S., HAMER, J.C., SAYLES, R.S., IOANNIDES, E. Surface damage effects caused by debris in rolling bearing lubricants, with an emphasis on friable materials. In: *Rolling element bearings — Towards the 21st century*, p. 1-8. Mechanical Engineering Publications, London, 1990

[20] PALMGREN, A. *Grundlagen der Wälzlagertechnik* [Foundations of antifriction-bearing technology], 3rd edition. Franckh, Stuttgart, 1964, 264 p.

[21] DOWSON, D., HIGGINSON, G.R. Elastohydrodynamics. *Proc. Inst. Mech. Eng.* 1967-1968, **182** (3A), p. 151-167

[22] HAMROCK, B.J., DOWSON, D. Isothermal elastohydrodynamic lubrication of point contacts — Part III — Fully flooded results. *J. Lubric. Technol*. 1977, **99**, p. 264-276

[23] IOANNIDES, E., HARRIS, T.A. A new fatigue life model for rolling bearings. *J. Tribol.* 1985, **107**, p. 367-378

[24] GABELLI, A., MORALES-ESPEJEL, G.E., IOANNIDES, E. Particle damage in Hertzian contacts and life ratings of rolling bearings. STLE Annual Meeting, Las Vegas, NV, 2005-05-15/19

[25] ISO 281:1990, *Rolling bearings — Dynamic load ratings and rating life*

ICS 21.100.20

Price based on 47 pages